JPL PUBLICATION 84-57

Science Opportunities Using the NASA Scatterometer on N-ROSS

M.H. Freilich

February 1, 1985

National Aeronautics and
Space Administration

Jet Propulsion Laboratory
California Institute of Technology
Pasadena, California

(597-200)

JPL PUBLICATION 84-57

Science Opportunities Using the NASA Scatterometer on N-ROSS

M.H. Freilich

February 1, 1985

National Aeronautics and
Space Administration

Jet Propulsion Laboratory
California Institute of Technology
Pasadena, California

(597-200)

The research described in this publication was carried out by the Jet Propulsion Laboratory, California Institute of Technology, under a contract with the National Aeronautics and Space Administration

National Aeronautics and
Space Administration

Washington, D.C.
20546

JAN 4 1985

eply to Attn of: EE

Dear Colleague:

Oceanography is a relatively new venture for NASA, with the first oceanic microwave sensor having flown aboard Skylab in 1972. Since that time, ocean-related sensors have flown aboard several satellites, most recently Seasat and Nimbus-7, both launched in 1978.

In the coming decade, NASA plans a series of spaceflight activities designed to further our understanding of ocean circulation, air-sea interactions, and the biological processes taking place in the upper ocean. This series--the NASA Scatterometer (NSCAT) to fly aboard the Navy Remote Ocean Sensing System (N-ROSS) satellite, the Ocean Topography Experiment (TOPEX, a dedicated altimeter mission), and a color scanner for a platform of opportunity--will also contribute to the World Climate Research Program, Global Habitability Program, and the International Geosphere/Biosphere Program.

I would like to take this opportunity to inform you that funding has been approved for NSCAT, the first element in NASA's planned series. Vector wind data from NSCAT has the potential for benefiting oceanography and meteorology, as well as making fundamental contributions to earth science. In addition, the understanding gained from the flight of NSCAT on N-ROSS will assist in the design of future operationally oriented observing systems for both the oceans and the atmosphere.

The enclosed Science Opportunities Document describes the capabilities of the NSCAT instrument and outlines various types of experiments that could be performed utilizing NSCAT data. The studies are designed to take advantage of the unique resolution, accuracy, and coverage of NSCAT vector wind data in order to allow models of oceanographic and meteorological processes to be developed and tested. I hope that this document will aid you and your colleagues in preparing to exploit the potential offered by NSCAT, and I invite you to share in the scientific planning and execution of this exciting project.

Sincerely,

S. G. Tilford

Shelby G. Tilford, Director
Earth Science and Applications Division
Office of Space Science and Applications

Abstract

A scatterometer (The National Aeronautics and Space Administration [NASA] Scatterometer [NSCAT]) will be flown as part of the Navy Remote Ocean Sensing System (N-ROSS) scheduled for launch in 1989. The NSCAT will provide frequent accurate and high-resolution measurements of vector winds over the global oceans. NSCAT data will be applicable to a wide range of studies in oceanography, meteorology, and instrument science. This document outlines the N-ROSS mission, describes the capabilities of the NSCAT flight instrument and an associated NASA research ground data-processing and distribution system, and surveys representative oceanographic, meteorological, and instrument science studies that may benefit from NSCAT data.

Acknowledgments

This document has benefited greatly from the contributions and suggestions by members of the Satellite Surface Stress Working Group, chaired by Professor J. J. O'Brien. Their magnum opus, *Scientific Opportunities Using Satellite Wind Stress Measurements Over the Ocean* (O'Brien, 1982), has served as a reference and guide during the preparation of this opportunities summary. Special thanks are due to D. Chelton, E. Harrison, K. Katsaros, L. McGoldrick, J. O'Brien, W. Pierson, P. Woiceshyn, M. Wurtele, and the members of the Jet Propulsion Laboratory NASA Scatterometer Project team.

Executive Summary

The atmosphere and the oceans interact in many complex ways. On the one hand, winds blowing across the ocean's surface generate surface waves, mix the waters in the upper ocean, and help to maintain the major current systems and general circulation of the ocean On the other hand, changing sea-surface temperature patterns, which often emerge in response to shifting winds, cause variations in both near-surface winds and the general circulation of the atmosphere. The oceans, then, with their vast supplies of heat and large heat constants, act as the flywheel of the coupled ocean-atmosphere system to determine regional and global climate.

Satellite observation systems are necessary to monitor and study large-scale motions in the atmosphere and the oceans. Past observational and modeling efforts, using data obtained by conventional means, have been severely hampered by a lack of accurate wind measurements with high resolution yet global coverage and a lack of frequent sampling coupled with records having long duration. The scatterometer flown on Seasat in 1978 clearly demonstrated that spaceborne microwave scatterometers were capable of obtaining the needed measurements of near-surface winds over the oceans.

The National Aeronautics and Space Administration (NASA) will provide a scatterometer as part of the Navy Remote Ocean Sensing System (N-ROSS) scheduled for launch in 1989. Although based on the Seasat design, the NASA Scatterometer will represent a significant advance in satellite microwave scatterometer technology. Specifically, an onboard digital doppler processor will allow colocation of backscatter cells from all antenna beams throughout the planned orbit, thus increasing both the accuracy and the coverage of the measurements. An additional antenna beam on each side of the subsatellite track will greatly increase the instrument's ability to determine unique wind directions. The planned three-year lifetime of the mission will allow investigations of longer term phenomena than was possible with the short Seasat mission.

In addition to its scatterometer flight instrument, NASA will provide a research ground data-processing and distribution system. This system will process the satellite data and produce several levels of geophysical wind products that will be archived and made available for use by science investigators.

The NASA Scatterometer data will be useful for a variety of studies in oceanography, meteorology, and air-sea interaction. Oceanographic studies include regional and global surface wave prediction, mixed layer modeling, and investigations of the dynamics of equatorial and midlatitude current systems. Meteorological and air-sea interaction studies involve the development of more accurate numerical weather-prediction and analysis models and include investigations of the mechanisms of tropical and extratropical cyclogenesis, of the response of the global atmospheric circulation to changes in the tropical oceans, and of the role of the atmosphere in the angular momentum balance of the earth.

Satellite Surface Stress (S^3) Working Group

James J. O'Brien, Chairman	The Florida State University
Janet Witte, Executive Assistant	Nova University
Robert Atlas	Goddard Space Flight Center
Emedio Bracalante	NASA/Langley Research Center
Otis Brown	University of Miami
Robert Haney	U.S. Naval Postgraduate School
D. Edmunds Harrison	Massachusetts Institute of Technology
Capt. David Honhart	U.S. Navy, Chief of Naval Operations Staff
Harley Hurlburt	Naval Oceanographic Research and Development Authority
Richard Johnson	Ocean Routes, Inc.
W. Linwood Jones	Satellite Television Corp.
Kristina Katsaros	University of Washington
Roger Lambertson	Control Data Corporation
Lawrence McGoldrick	Applied Physics Laboratory/Johns Hopkins University
Richard Moore	University of Kansas
Steven Peteherych	Atmospheric Environment Service, Canada
Willard Pierson	The City College of the City University of New York
James Price	Woods Hole Oceanographic Institution
Duncan Ross	NOAA-Atlantic Oceanographic and Meteorological Laboratory
Robert Stewart	Jet Propulsion Laboratory and Scripps Institution of Oceanography
Frank Wentz	Remote Sensing Systems
Peter Woiceshyn	Jet Propulsion Laboratory
Morton Wurtele	University of California, Los Angeles

Acronyms

AAFE RADSCAT	Advanced Aerospace Flight Experiment Radiometer/Scatterometer
ACC	Antarctic Circumpolar Current
DMS	Data management system
DMSP	Defense Meteorological Satellite Program
ENSO	El Niño – Southern Oscillation
FNOC	Fleet Numerical Oceanography Center
GDR	Geophysical data record
GOASEX	Gulf of Alaska Experiment
ITCZ	Intertropical convergence zone
JASIN	Joint Air-Sea Interaction Experiment
JPL	Jet Propulsion Laboratory
JSC	Johnson Space Center
NASA	National Aeronautics and Space Administration
NCAR	National Center for Atmospheric Research
NDBC	National Data Buoy Center
NOAA	National Oceanic and Atmospheric Administration
NRCS	Normalized radar cross section
NRL	Naval Research Laboratory
N-ROSS	Navy Remote Ocean Sensing System
NSCAT	NASA Scatterometer
NWP	Numerical weather prediction
PBL	Planetary boundary layer
PODS	Pilot Ocean Data System
S^3	Satellite Surface Stress
SASS	Seasat-A Satellite Scatterometer
SDR	Sensor data record
SMMR	Scanning Multichannel Microwave Radiometer
SNR	Signal-to-noise ratio
SSM/I	Special Sensor Microwave/Imager
SST	Sea-surface temperature
TOGA	Tropical Ocean/Global Atmosphere Experiment
TOPEX	Ocean Topography Experiment (proposed altimetric satellite)
TWTA	Traveling wave tube amplifier
WOCE	World Ocean Circulation Experiment

Contents

Figures

Table

Section I
Introduction

Satellite scatterometers can provide frequent, accurate, high-resolution measurements of surface vector winds over the global oceans. Such scatterometer data will play an increasingly large role in a variety of oceanographic and meteorological studies ranging from weather and wave prediction to investigations of the long-term variability of climate and ocean-current systems. The global nature of these scatterometer wind measurements will make them especially valuable to planned large-scale experiments such as the World Ocean Circulation Experiment (WOCE) and Tropical Ocean/Global Atmosphere (TOGA).

This document describes the capabilities of a scatterometer (the National Aeronautics and Space Administration [NASA] Scatterometer [NSCAT]) to be flown as part of the Navy Remote Ocean Sensing System (N-ROSS) as well as an associated NASA ground data-processing and distribution system. A representative survey of possible oceanographic and meterological studies using scatterometer data forms the latter half of this document. Many of these studies were identified in the report of the Satellite Surface Stress (S^3) Working Group (O'Brien, 1982), which served as a guide for the preparation of this document. Potential investigators are urged to evaluate the possible utility of NSCAT data for their specific oceanographic and meteorological studies.

A. The Need for Satellite Scatterometry

The temporal and spatial distributions of fluxes of radiation, kinetic energy, heat, and momentum between the atmosphere and the oceans greatly influence near-surface oceanic and atmospheric motions. The vertical flux of horizontal momentum due to winds blowing over the oceans ("wind stress") is the largest single input of momentum to the oceans. Winds thus play a crucial role in generating surface and internal waves, in mixing the upper ocean, and in establishing and maintaining currents and large-scale oceanic circulation. Winds over the oceans also strongly influence and modulate the transfers of kinetic energy, heat, and moisture between the air and the sea.

Just as winds are directly or indirectly responsible for a wide range of oceanic phenomena, so the properties of the upper ocean, notably sea-surface temperature, strongly influence atmospheric motions. Meteorological interest in oceanic winds stems in large part from the need to understand the many ocean-atmosphere interrelationships which define regional and global climate. In addition, a major source of error in predicting atmospheric motions and weather is the incomplete knowledge of the *present* state of the atmosphere. Oceans account for 70% of the earth's surface; therefore, accurate knowledge of the winds over the oceans is crucial to our ability to define the state of the atmosphere in a global sense.

Deficiencies in existing large-scale wind data sets have severely hampered past studies of both the ocean's response to wind forcing and the interactions between the ocean and the atmosphere. While these studies require nearly simultaneous, high-resolution wind data over large areas and for long periods of time, conventional wind measurements from ships, buoys, and islands are sparsely and irregularly distributed over the global oceans (Fig. 1). Measurements from merchant ships are notoriously inaccurate, while data obtained from islands and coastal stations may not be representative of open ocean conditions due to orographic contamination.

Instruments mounted on polar-orbiting satellites can provide data with the coverage and spatial resolution required for the study of many oceanographic and atmospheric phenomena. Moore and Pierson (1966) first suggested the use of a satellite-borne active microwave scatterometer for the global measurement of oceanic winds. Although satellite-borne active and passive systems (altimeters, radiometers, and scatterometers) have subsequently been used to measure wind *speed*, scatterometers have demonstrated clear superiority because they can measure *vector* winds (both speed and direction).

B. History of Wind Measurement by Scatterometers

The major efforts leading to the current design of the NSCAT system are summarized below. A more complete review of the historical development of scatterometer systems to measure surface winds over the ocean can be found in Moore and Fung (1979).

The use of active microwave systems for measuring oceanic winds resulted from the development in World War II of radar systems for air defense: the causes of "sea clutter" were intensely researched in the U.S. and Britain following the end of World War II. Experimental studies (Wiltse et at., 1957; Grant and Yaplee, 1957; Campbell, 1959) in the 1950s and early 1960s established an apparent correlation between near-surface wind speed and the normalized radar cross section (σ_0) of the ocean at moderate incidence angles (the vertical angle between the normal to the surface and the illuminating radiation).

Extensive series of airborne measurements by the Naval Research Laboratory (NRL), utilizing a four-frequency pencil-beam scatterometer, and by NASA/Johnson Space Center

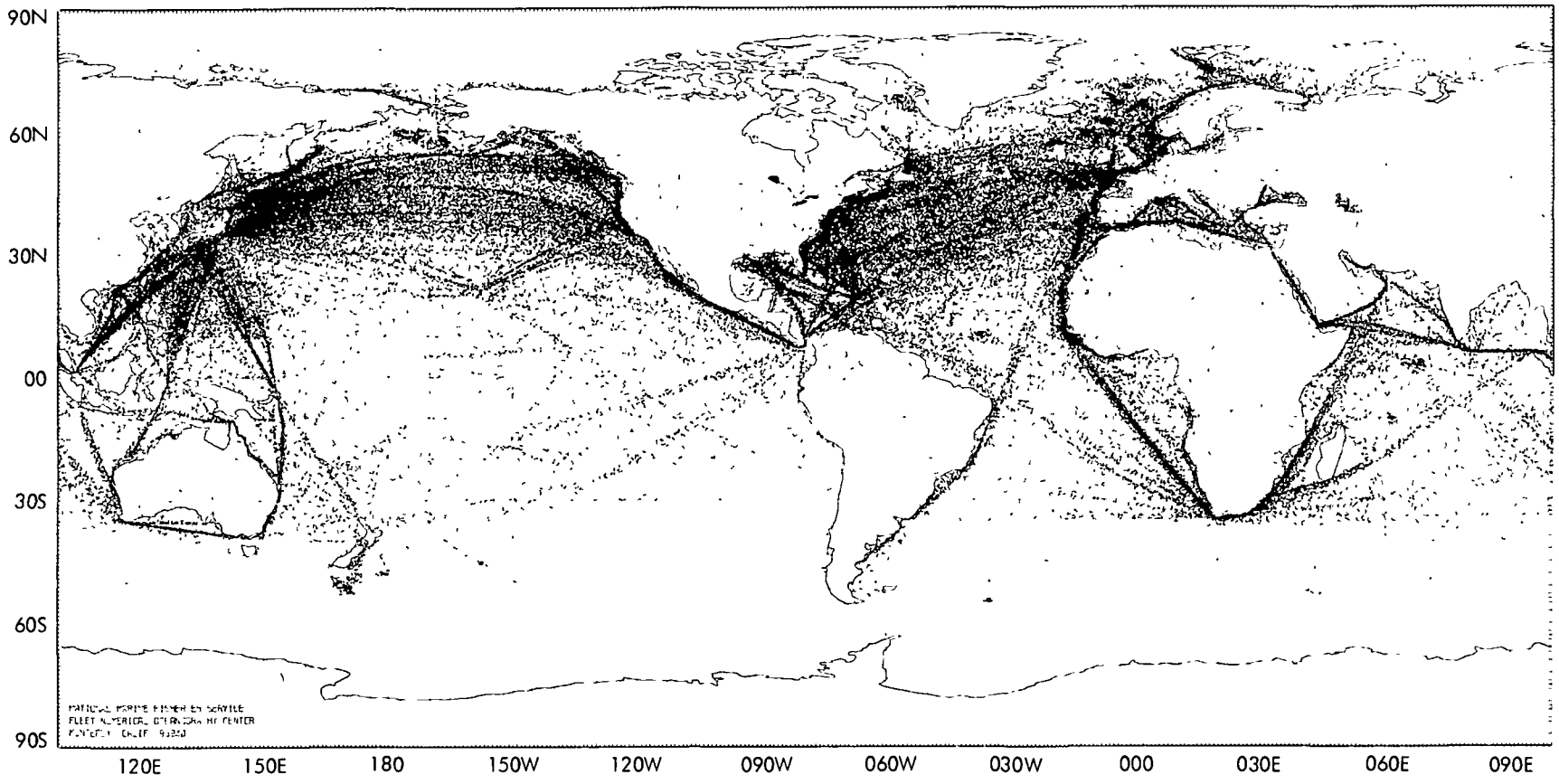

Fig. 1. Locations of all ship observations of surface meteorological variables for the period 1 July 1978 to 9 October 1978. Each dot represents a single ship observation (dots on land are due to incorrect reporting of ships' positions). Note that the observations are mostly confined to the Northern Hemisphere and to major shipping lanes. The Seasat Scatterometer obtained nearly 15 million wind observations in the same period, as compared with 119,000 observations from ships. (Courtesy of D. McLain, NMFS)

(JSC), utilizing an airborne fan-beam scatterometer at Ku-band frequency, established an empirical power-law dependence of σ_0 on wind speed (Valenzuela et al., 1971; Newton and Rouse, 1972). However, instrument calibration uncertainties prevented comparing data from different experiments, and the data were incorrectly interpreted to suggest that σ_0 tended to saturate at high wind speeds.

In the early 1970s NASA developed an improved pencil-beam aircraft scatterometer, the Advanced Aerospace Flight Experiment Radiometer/Scatterometer (AAFE RADSCAT); it was stable and demonstrated good absolute calibration (Jones et al., 1977). Field experiments were conducted that refined the power-law relationship between σ_0 and wind speed at incidence angles from 20° to 70° (Fig. 2). In addition, data

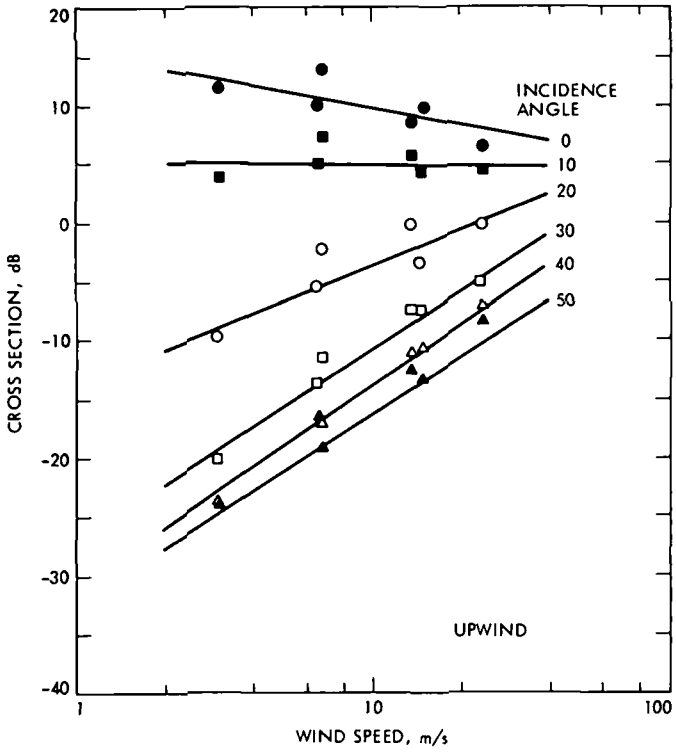

Fig. 2. Scattering cross section per unit area (σ_0) for 13.96 GHz vertical polarization, as a function of incidence angle and wind speed (adapted from Jones, Wentz, and Schroeder, 1978)

acquired while the aircraft flew in circular patterns allowed the examination of the relationship between σ_0 and azimuth angle χ, the horizontal angle between the radar illumination and the wind direction (Jones and Grantham, 1975, Jones et al., 1977, Jones and Schroeder, 1978). It was found that σ_0 (in dB) varied approximately as $\cos(2\chi)$ (where the quantity $\chi = 0$ [π] corresponds to upwind [downwind]) and that the amplitudes of the modulations varied with incidence angle, wind speed, and polarization (Fig. 3). It is the nearly harmonic variation of σ_0 with azimuth angle that allows satellite scatterometers to determine wind speed *and* direction by measuring σ_0 from a given area of the sea surface at multiple azimuth angles.

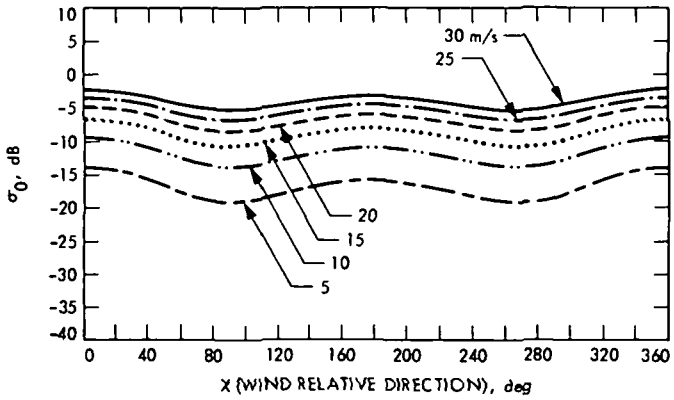

Fig. 3. The σ_0 dependence on azimuth angle and wind speed (from the SASS-I geophysical model function, horizontal polarization, 30° incidence angle; adapted from Boggs, 1982)

The first spaceborne radiometer/scatterometer was flown aboard the Skylab missions SL2, SL3, and SL4 in 1973-1974 (Young and Moore, 1977). Many measurements of σ_0 were obtained at various incidence angles for a wide range of wind conditions. Since the scatterometer employed a single pencil beam, only a single measurement of σ_0 at one (unknown) value of the azimuth angle was obtained from each area on the sea surface. Because σ_0 varies with azimuth angle, independent knowledge of the wind direction was necessary to infer wind speed from the measured σ_0. Although the Skylab experiment demonstrated that spaceborne scatterometers were indeed feasible, the lack of high-quality surface wind measurements for comparison with Skylab measurements greatly detracted from the scientific quality of the scatterometer data.

Additional experiments with the airborne AAFE RADSCAT in the mid 1970s led to a further refinement of the empirically based geophysical model function used to relate σ_0 to surface wind speed as a function of incidence angle and azimuth angle. Ross and Jones (1978) showed that scatterometer estimates of wind speed were relatively insensitive to surface gravity wave conditions, while Jones and Schroeder (1978) suggested that σ_0 might be more highly correlated with surface *stress* (expressed as friction velocity) than with actual wind velocity at a fixed anemometer height.

The Seasat-A Satellite Scatterometer (SASS), a fan-beam, dual-polarized, Ku-band scatterometer, was flown aboard the Seasat satellite from June to October, 1978. The four antennas (two on each side of the spacecraft) allowed measurements of

σ_0 at two azimuth angles (one from the fore antenna, one from the aft) with spatial resolution of approximately 50 km, in two swaths approximately 600-km wide on each side of the subsatellite track. The σ_0 measurements from the fore and aft beams were combined to provide estimates of wind speed and up to four possible directions. A multifrequency radiometer (the Scanning Multichannel Microwave Radiometer [SMMR]) was used to correct some measurements for the small effects of liquid atmospheric water The world's ice-free oceans were sampled frequently during the three-month lifetime of Seasat. Some results of studies based on SASS data are described in detail in Appendix A; below are listed only major accomplishments.

(1) SASS demonstrated that accurate (±2 m/s) measurements of wind speed and direction (up to four possible directions, one of which was correct to within ±20°) could be obtained from satellite scatterometer data alone.

(2) The geophysical model function was further refined by comparing SASS data and high-quality *in situ* data obtained in the Joint Air-Sea Interaction and the Gulf of Alaska Experiments (JASIN and GOASEX, respectively)

(3) SASS data were used to construct the first global, nearly synoptic maps of surface-wind speed and direction (Fig. 4).

The NASA Scatterometer, NSCAT, while similar to SASS, will have enhanced capabilities:

(1) An additional antenna on each side of the subsatellite track will reduce the number of directions associated with nearly every wind speed to 2, nearly 180° apart.

(2) An onboard digital doppler processor will allow coregistration of σ_0 measurements from different antennas over the entire swath width.

(3) The quantity σ_0 will be measured with a spatial resolution of approximately 25 km.

(4) A dedicated NASA ground data-processing and distribution system will provide research quality data to the science community in a timely fashion

(5) The expected 3-year lifetime of NSCAT will allow for some studies of seasonal and interannual variations.

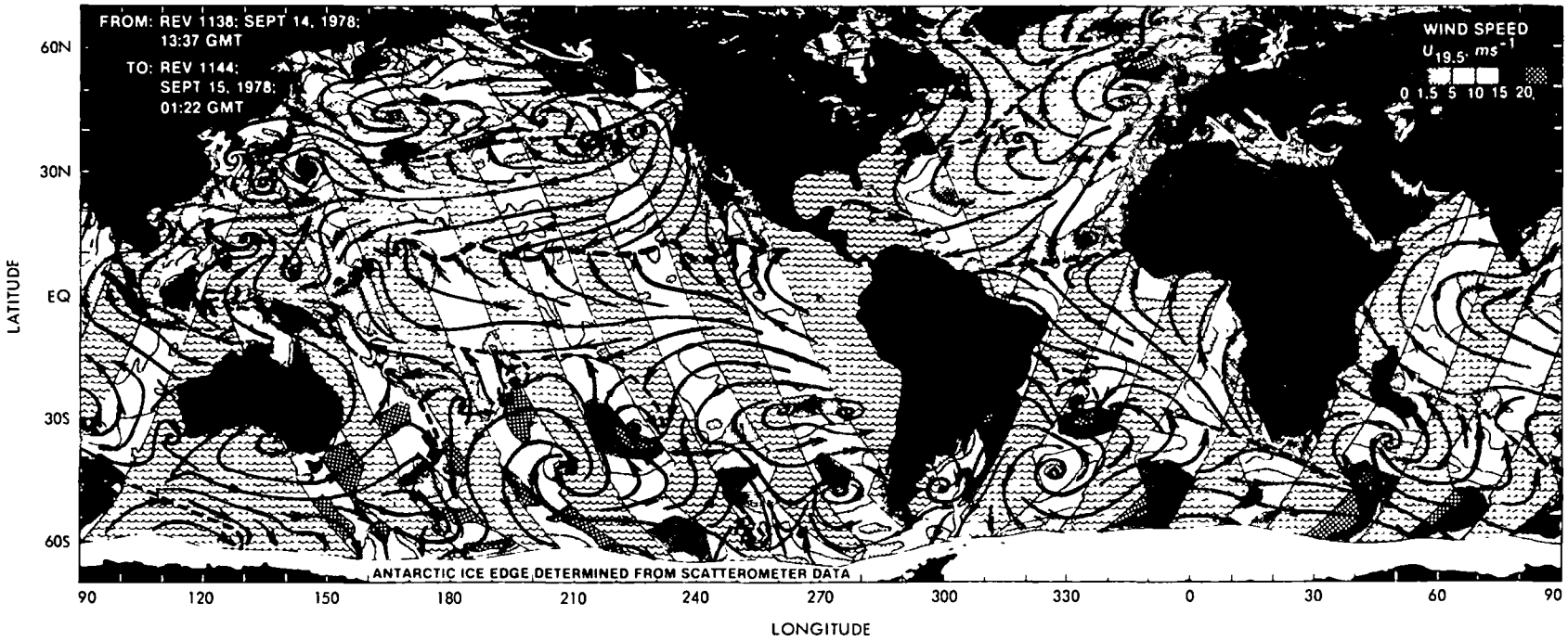

Fig. 4. The analysis and map of global oceanic winds from Seasat SASS data for 14–15 September 1978. Wind speeds measured by SASS are shown by stippling within the SASS swaths. Dark arrows are approximate streamlines inferred from SASS data and other *in situ* and satellite data. Dashed lines mark the positions of surface convergence zones and fronts (adapted from Peteherych et al., 1984).

Page intentionally left blank

Page intentionally left blank

Section II
N-ROSS Mission Description

N-ROSS is a satellite system designed to provide frequent, accurate, high-resolution measurements of near-surface wind, ocean topography, wave height, sea-surface temperature, and atmospheric water content over the global oceans. The design, implementation, launch, and operation of the N-ROSS mission will involve interagency collaboration between the Navy, NASA, the National Oceanic and Atmospheric Administration (NOAA), and the Air Force. Drawing on experience gained in the design and implementation of SASS, NASA will provide the scatterometer flight instrument as well as a research ground data-processing and distribution system. In all, N-ROSS will have four microwave instruments mounted on a single satellite in a near-polar orbit:

(1) A scatterometer (described more fully in Section III).

(2) A microwave altimeter, similar to that flown on Seasat, to measure ocean topography and significant wave height.

(3) A Special Sensor Microwave/Imager (SSM/I), a four-frequency (19, 22, 37, and 85 GHz) scanning microwave radiometer, that will be used to acquire data on sea-surface temperature, scalar wind speed, atmospheric water content, and ice characteristics.

(4) A low-frequency (5.2 and 10.4 GHz) scanning microwave radiometer that, in conjunction with SSM/I data, will be used to measure sea-surface temperature with a resolution of 25 km.

A schematic diagram of the proposed locations and orientations of the four instruments is shown in Fig. 5. Figure 6 illustrates the measurement swaths of the instruments.

Although final mission parameters have not yet been fully established, present plans call for N-ROSS to be launched aboard a Titan-II rocket in mid-1989. N-ROSS will be placed in a sun-synchronous orbit at an altitude of approximately 830 km and an inclination angle of 98.7°. The designed mission duration is three years.

Data from the N-ROSS mission will be transmitted to the Fleet Numerical Oceanography Center (FNOC) in Monterey, California. Raw NSCAT data, orbit and attitude data, and earth-located SSM/I brightness temperatures (corrected for antenna pattern biases) will be provided to the NSCAT research ground data-processing system by the Navy. As described in Section III.C, NASA will process all usable scatterometer data collected over the ocean and will distribute scatterometer data (at various levels of processing) and some SSM/I data to scientific users in a timely fashion. Reduction, analysis, and dissemination of other N-ROSS data (altimeter and radiometer data) will not be carried out under the auspices of the NSCAT project.

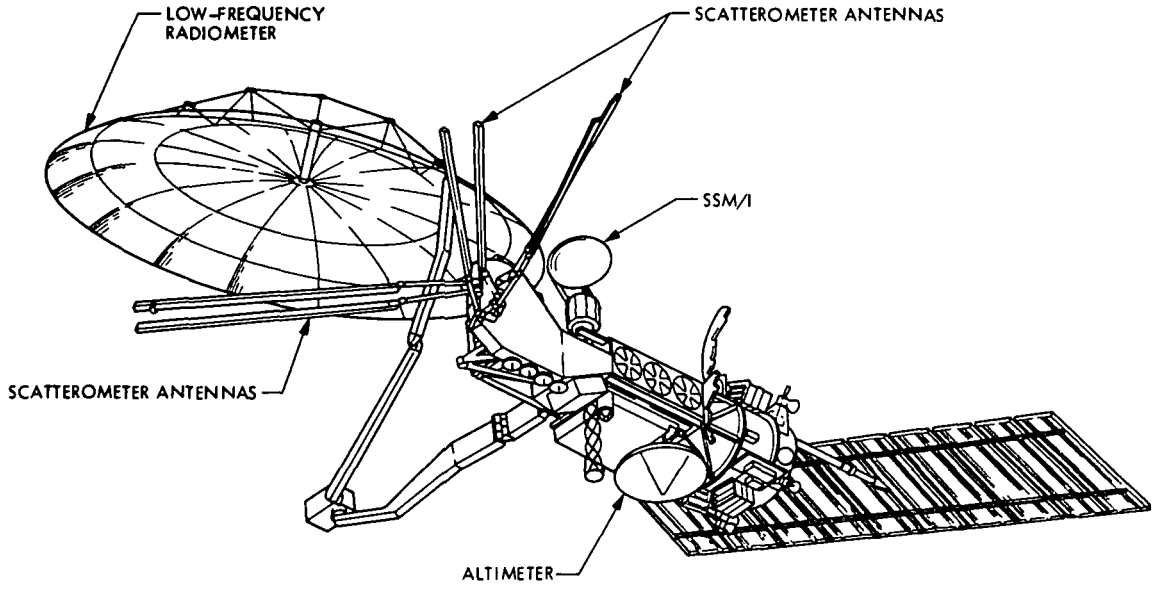

Fig. 5. Schematic configuration of the N-ROSS spacecraft, showing the locations of the scatterometer, SSM/I, low-frequency radiometer, and altimeter antennas

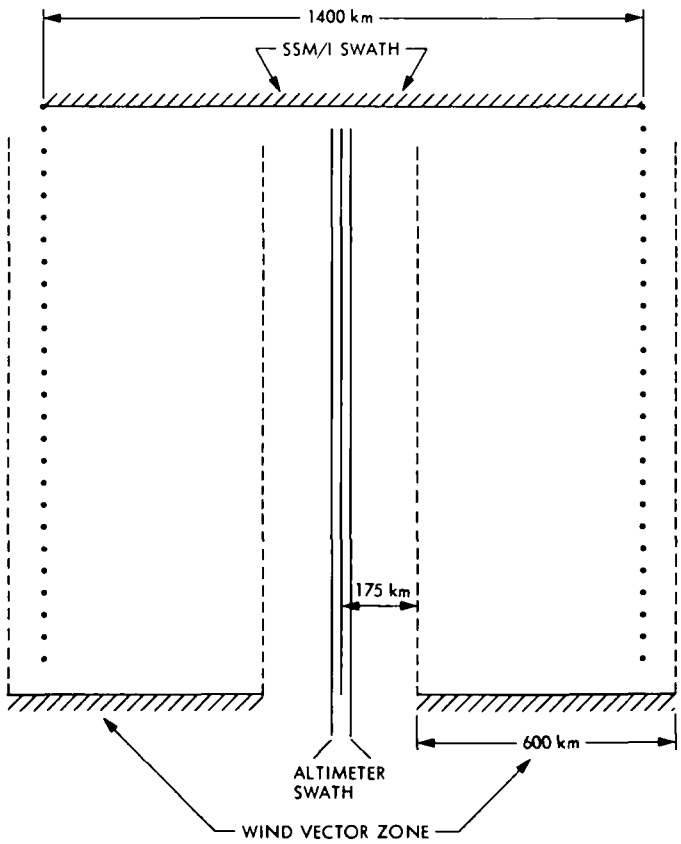

Fig. 6. Plan view of N-ROSS measurement swaths on the earth's surface. Swath widths are drawn to scale. Details of the measurement swath for the high-resolution radiometer are not yet known.

Section III
NASA Scatterometer System

The baseline design for the NASA scatterometer system is described below. Although the detailed information presented in the following subsections is current as of the printing of this document, minor changes may be made in the final design and implementation phases of the instrument, research ground data-processing system, and validation activities.

A. Requirements and Capabilities

Performance requirements for the NSCAT system were established by the S^3 Working Group (O'Brien, 1982) and the N-ROSS Project (Jet Propulsion Laboratory, 1983). During the definition study (Phase A) conducted at the Jet Propulsion Laboratory (JPL) in 1983, the requirements were further refined and reviewed by the S^3 Working Group and the N-ROSS Project. The following summarizes the performance requirements for the NSCAT flight instrument and its associated research ground data-processing system.

1. Wind Speed Accuracy

The rms accuracy will be better than the greater of 2 m/s or 10% of the true wind speed in the range from 3 to 30 m/s. If the geophysical model function remains valid for winds greater than 30 m/s, the system will be capable of measuring winds up to 100 m/s.

2. Wind Direction Accuracy

At least 90% of the wind vectors retrieved will have no more than two directional ambiguities which subtend angles of 150° to 210°. The wind direction rms accuracy will be 20° or better for the one ambiguity closest to the true wind. The research ground data-processing system will employ an objective algorithm to choose a unique wind direction associated with each speed solution

3. Rain Flag

Based on SSM/I data, a flag will be present on σ_0 and vector-wind cells where the presence of liquid atmospheric water would degrade the vector-wind measurement such that wind speed and direction accuracy requirements would not be met (see subsections III.A 1 and III.A.2). Cells for which there are no usable SSM/I data will be identified by a separate flag.

4. Spatial Resolution

The σ_0 measurements will be obtained with a resolution of 25 km (the distance between centers of adjacent cells along an antenna beam). For NASA users, winds will be processed with a resolution of 50 km (each retrieved wind vector will characterize the winds within a square, 50 km on each side; see Fig 7).

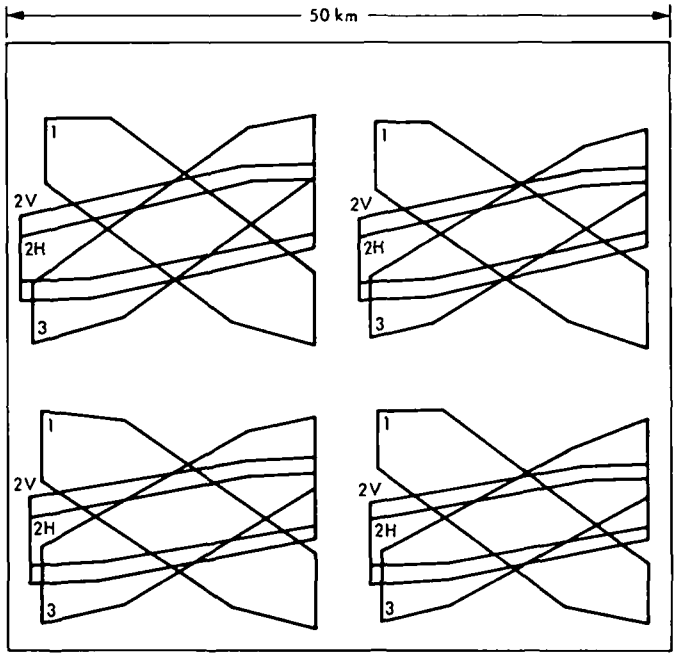

Fig. 7. Plan view showing the 16 σ_0 cells used to construct a 50 km × 50 km wind vector resolution cell

5. Wind Vector Cell Location Accuracy

Cell centers of 50-km wind cells will have an absolute location accuracy of better than 50 km (rms). The relative location of any two adjacent wind-cell centers will be better than 10 km (rms).

6. Coverage

Vector winds over at least 90% of the global ice-free oceans will be obtained at least once in every two-day period.

7. Data Reduction and Distribution

All wind data collected over the ocean will be processed within two weeks after timely (seven days from satellite acquisition) reception from the N-ROSS Project. Raw data will be processed to vector winds, and the vector winds will be combined into wind-field maps. All raw data, as well as selected levels of processed data, will be archived for the duration of the mission. All ocean vector-wind data and wind-field maps will be made available to users via an on-line data-management system.

B. Instrument Description

The NSCAT flight instrument utilizes design concepts similar to those used for SASS. Pulses of radiation at a microwave

frequency of 13.995 GHz are emitted, and then the normalized radar cross section (σ_0) of the ocean is determined by accurately measuring the backscattered power. The σ_0 measurement, in turn, can be related to the local winds. Measurements of σ_0 are obtained in swaths approximately 600-km wide on each side of the subsatellite track. The swath coverage will allow winds over ~90% of the ice-free oceans to be observed in each two-day period (see Fig. 8[a]; Fig. 8[b] provided for comparison). A more complete description of the principles of scatterometry can be found in Appendix B.

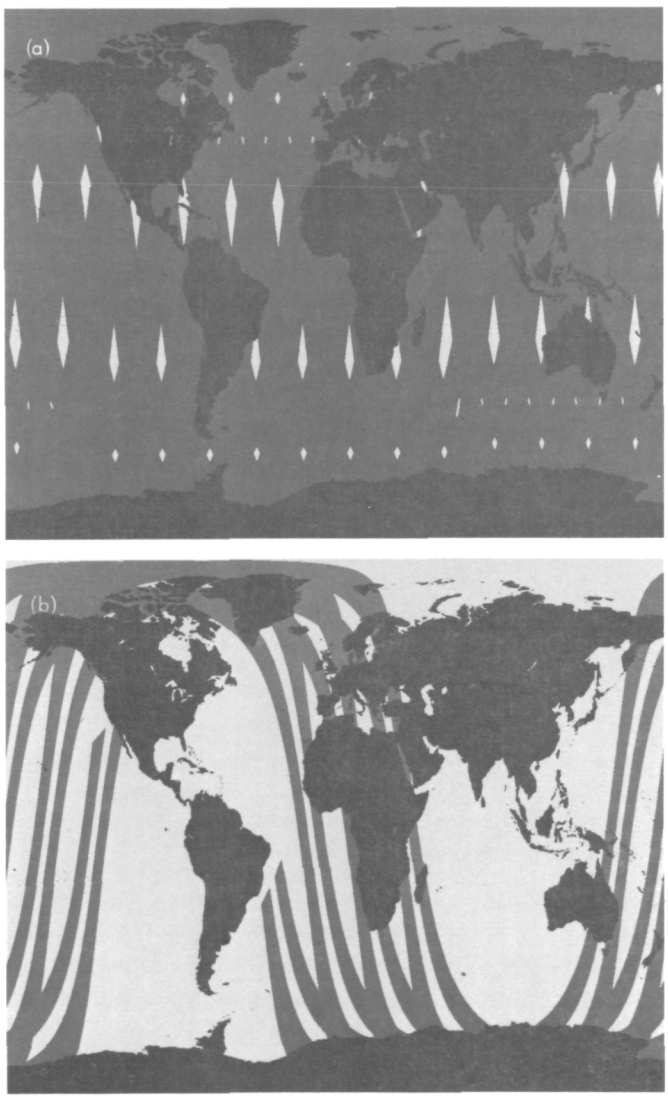

Fig. 8. NSCAT coverage over time: (a) after 2 days. Gray areas are regions in which vector wind measurements have been made at least once during the 2-day period. White areas denote regions that have not been covered by the NSCAT wind measurement swath. Approximately 90% of the oceans are covered at least once every 2 days; (b) after 6 orbits. Gray and white areas represent regions in which wind vector measurements have taken place. Note that some high-latitude regions are sampled more than once.

1. Physical Subassemblies

The flight instrument is composed of three major subassemblies: an RF subassembly, the antennas, and a digital subassembly. The RF subassembly contains the transmitter and receiver subsystems. The antennas generate a fan-like beam and produce the ground-illumination geometry shown in Fig. 9. The digital subassembly contains both the doppler-processing subsystem used to achieve along-beam (incidence angle) resolution and the control and logic subsystems for the instrument.

2. Functional Subsystems

Figure 10 shows a schematic block diagram of the NSCAT flight instrument. The information below describes several of the major subsystems.

a. **Transmitter.** The transmitter subsystem employs a traveling wave tube amplifier (TWTA) to generate radar pulses at 13.995 GHz. The pulses are ~5 ms in duration. A single antenna cycle consists of a series of 25 pulses (each followed by an approximately 16-ms receiving interval), followed by a 64.6-ms noise measurement interval (Fig. 11). This pattern is repeated cyclically for each antenna beam. The peak pulse power is approximately 100 W.

b. **Receiver.** A portion of the backscattered signal is captured by the antennas during the 16-ms receiving interval following each transmitted pulse and is then amplified by a low-noise amplifier. The amplified signal is made up of the desired backscattered signal as well as "noise" due to both the intrinsic system noise and the natural microwave emissivity of the

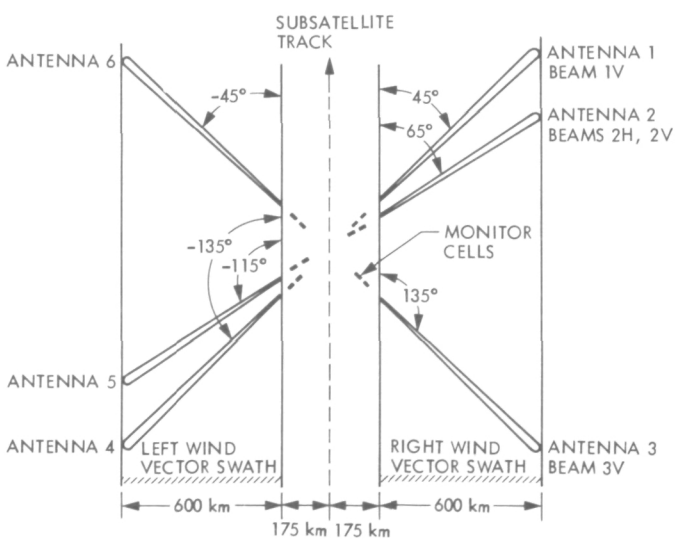

Fig. 9. Schematic plan view of the illumination patterns of the antennas on the earth

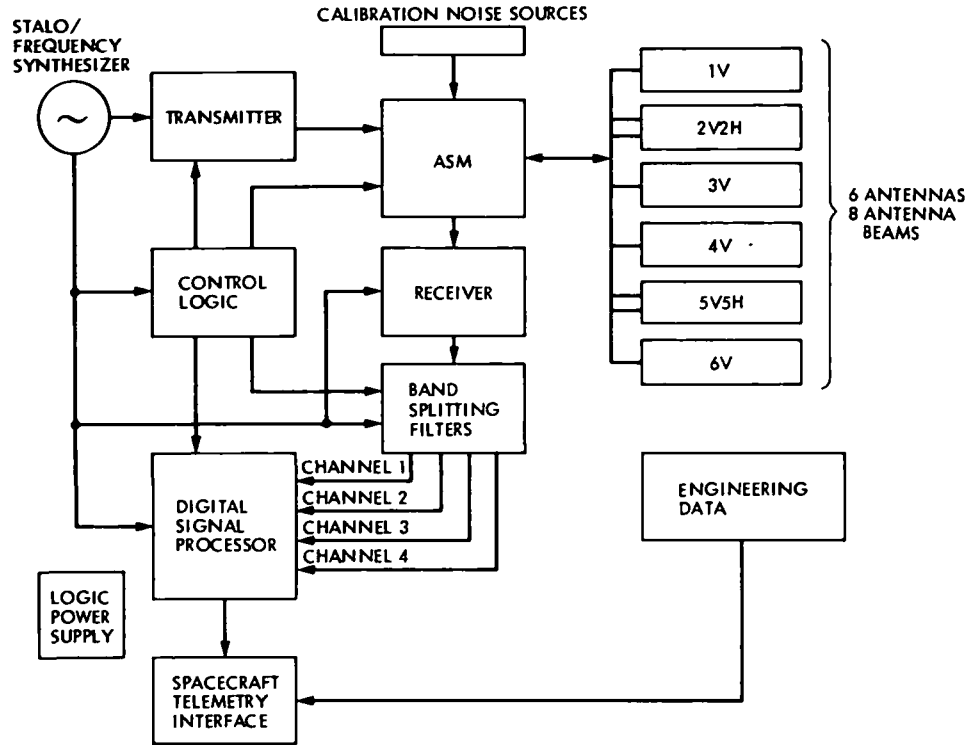

Fig. 10. Schematic block diagram of the NSCAT flight instrument

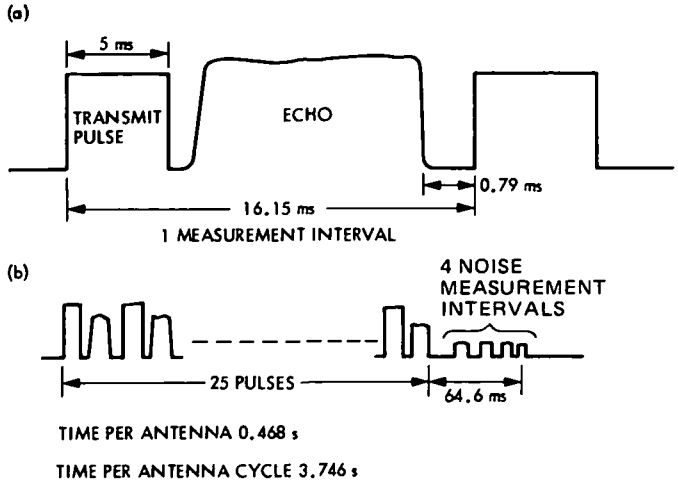

Fig. 11. Timing diagram: (a) Transmit and receive timing; and (b) 25 transmit/receive cycles followed by a 64.6-ms receive-only period comprising a full cycle on a single antenna

ocean. In order to extract the desired backscatter signal from the amplified signal, the unwanted noise power must be estimated and properly subtracted. This is accomplished in the 64.6-ms "receive-only" period following each cycle of 25 transmitted pulses.

c. **Antenna.** The antenna subsystem is made up of 6 antennas, shown schematically in Figs. 5 and 9. Each of the physical antennas is approximately 3-m long, and each generates a fan-like beam that is narrow (~0.5°) in the across-beam dimension and wide (~25°) in the along-beam dimension. (Due to the curvature of the earth, the incidence angle range sampled by the fan-beam geometry is from approximately 10° to 60°.) On deployment, the antennas are tilted and rotated relative to the spacecraft to produce the ground-illumination geometry shown in Fig. 9. In the baseline design, each fore and aft antenna on either side of the spacecraft (labeled 1, 3, 4, and 6 in Fig. 9) generates a single, vertically polarized beam. Each middle antenna (labeled 2 and 5) generates two beams, one vertically polarized, and one horizontally polarized.

d. **Digital processor.** The received signals are processed by an onboard digital processor in order to achieve along-beam resolution. The basis of the processor's operation is that the satellite's motion and the earth's rotation cause a doppler shift in the received signal. This shift is a function of along-beam distance. Thus, the backscattered power from a selected along-beam area can be obtained by filtering the signal within a chosen band of doppler-shift frequencies. The doppler-processing subsystem uses adjustable center frequencies in order to allow colocation of cells from all antennas (fore,

middle, and aft) everywhere in the spacecraft's orbit This digital doppler-processing system on NSCAT represents a significant improvement over the SASS fixed analog filter system. The adjustable center frequencies of the NSCAT digital processor will allow vector-wind measurements to be made over the entire swath everywhere in the planned NSCAT orbit, thus increasing the coverage over that achieved by SASS (Due to the effects of the earth's rotation, the fixed filter system on SASS achieved full swath coverage only at the extreme high-latitude portions of the orbit) In addition, more accurate colocation of σ_0 cells from different antenna beams on NSCAT will greatly simplify the ground processing used to retrieve vector winds as well as provide for more accurate wind measurements in regions with large gradients in wind speed and direction.

C. NSCAT Data-Processing System

As part of the NSCAT program, JPL will implement and operate a research ground data-processing and distribution system for NASA research users. This system will produce several levels of wind products and will distribute data to users in a timely manner.

The NSCAT data-processing system will provide dedicated, nonreal-time processing of scatterometer data for research users. The system will be designed to process all ocean data with no backlog and will be tested and ready for use at launch. Management and distribution of the data will be provided by an on-line archiving system such as the Pilot Ocean Data System (PODS).

1. Data Processing and Products

It is assumed that the Navy will provide the data-processing system with all available time-ordered frame-synchronized raw scatterometer data, N-ROSS orbit and attitude data, and ground-located SSM/I-brightness temperatures within three days of data acquisition. This integrated data package will be all that will be necessary to produce the desired wind products. After an initial six-month shakedown period following launch, data will be available to users two weeks after JPL receives the raw data

Data processing will proceed through several levels (see Fig. 12). The detailed definitions of the various data levels are shown in Table 1 Raw data are referred to as Level 0 After data cleanup, conversion from binary to engineering units, earth location, and backscatter computation, the normalized radar backscatter cross section that is referred to as Level 1 5 will be obtained These data are the primary physical measurements of the scatterometer system and constitute the sensor data record (SDR). All usable data received from FNOC will be processed to Level 1.5. After earth location, the data will be flagged as to whether the cell is ocean or nonocean (land or ice).

The data-processing system will receive earth-located SSM/I brightness temperatures (Level 1.5) from FNOC. These data, where available, will be used to produce a rain flag for σ_0 cells Because the SSM/I swath does not completely cover the scatterometer swath, some σ_0 cells cannot be flagged. A "no information" flag will be used for these cells

As shown in Fig. 7, sixteen σ_0 measurements (each with 25-km resolution) will be combined into 50-km squares for wind retrieval. Each cluster of four σ_0 cells in Fig. 7 represents colocated σ_0 measurements from each antenna beam (vertical polarization from the fore, middle, and aft antennas; horizontal polarization from the middle antenna only).

Extensive simulation studies have shown that multiple vector wind solutions are obtained when the sixteen σ_0 measurements are processed. These solutions are found to have similar speeds but varied directions. In contrast to the SASS case, the polarization mix and antenna beam angles on NSCAT will allow the multiple vector wind solutions to be ordered by the relative likelihood of their being the correct solution. This ordering does not depend in any way on additional *in situ*

Table 1. Data level definitions

Level	Definition
0	Raw data, frame synchronized, gap filled, time ordered and nonredundant (obtained from the Navy)
1 0	Decommutated data in engineering units
1 5	Sensor data record (SDR)· Data in sensor units (earth-located σ_0).
2 0	Data in geophysical units (vector wind speed and direction) with 6 or fewer solutions at each location Two solutions, at least 150° apart, will have probabilities greater than 90% of being the correct solution.
2 5	Geophysical data record (GDR) As 2 0 but with a single wind speed and direction at each location. Wind solutions are tagged with algorithm, time, location, and quality flags.
3 0	Wind map, 1° × 1° earth-fixed grid map of vector-averaged winds Vector averages are over all wind vector solutions falling within each spatial grid during the preceding two-day period

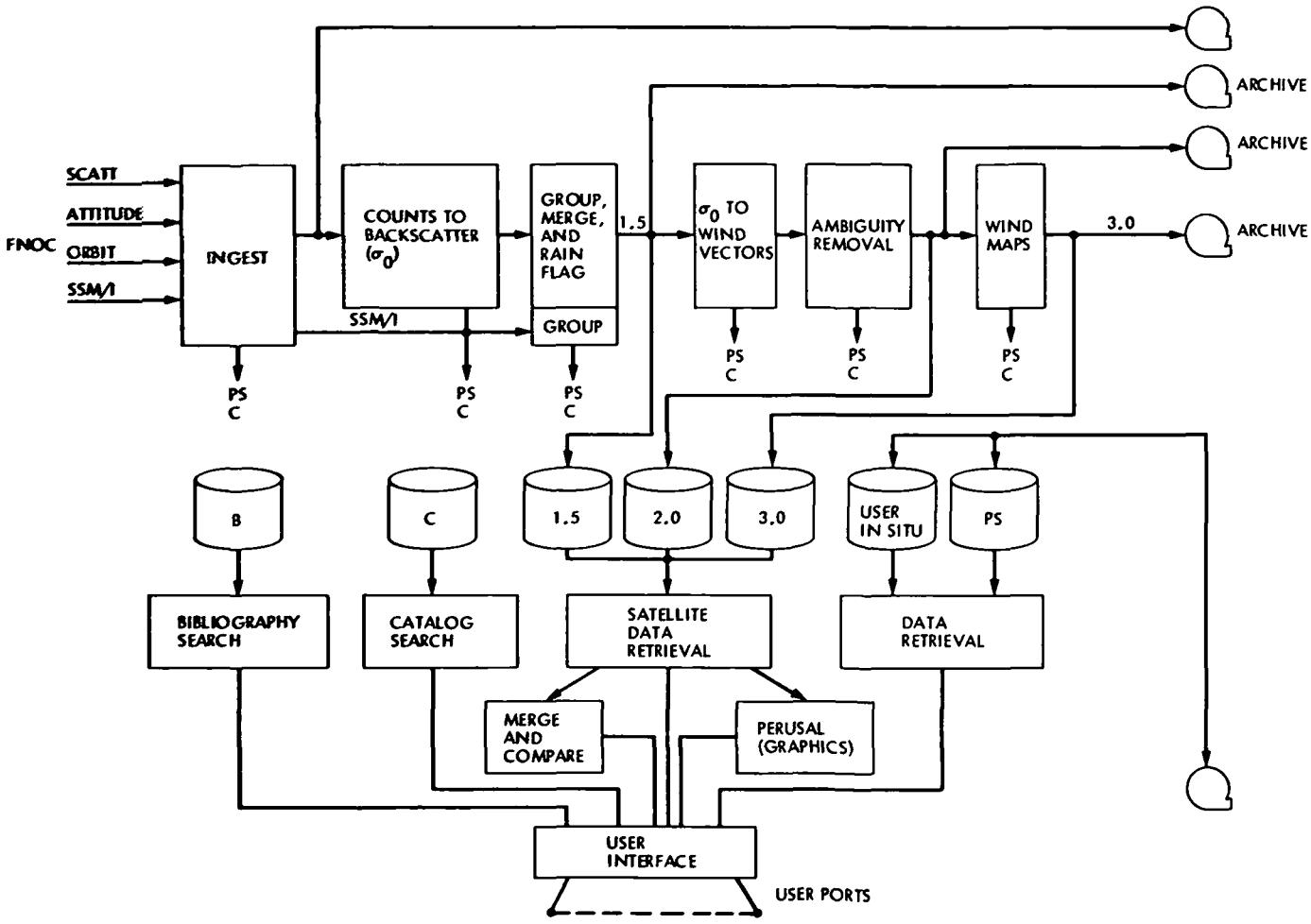

Fig. 12. Schematic diagram of the NSCAT data-processing system. Numbers (e.g. 1.5, 2.0) represent levels of processing as discussed in Subsection III.C.1. "PS" stands for "Performance Summary"; "C" stands for "Catalog entry."

information. The wind data with multiple solutions are referred to as Level 2.0.

The multiple wind solutions with their associated relative likelihoods will be used as input to an iterative objective scheme for selecting unique wind directions. The relative likelihoods of the solutions in a cell and the directions selected for its neighbors will be used to select a unique direction for each wind retrieval cell. The resulting unique vector winds at 50-km resolution will be referred to as Level 2.5 data. Simulations indicate that the highest likelihood direction points in the direction of the true wind at least 70% of the time. It is expected that the ambiguity removal scheme will select the vector wind solution that points closest to the direction of the true wind more than 90% of the time. The ambiguity removal algorithm is currently under development at JPL. Exact specifications of the algorithm performance will be available in early 1985.

To provide easy access to the wind data, a wind-field map product will be produced. This product will consist of daily maps with $1^\circ \times 1^\circ$ resolution in longitude and latitude. Each map will be produced from the previous two days' data. Every $1^\circ \times 1^\circ$ cell will contain the vector average of all wind vectors falling in the cell over the two-day period. These maps are not intended for direct scientific analysis but rather for aiding data selection. Areas in which there are no data during the two-day period will be indicated. All usuable ocean data will be processed to maps. The mapping algorithm is currently under development at JPL, and the requirements of NASA research users will be evaluated in defining the final form of the wind-field maps.

In addition to processed data, summaries of system performance will be produced. These will allow the checking of instrument health, data system throughput, and gross statistics of the wind data.

2. Data Management and Distribution

Data will be available to users through a data management system (DMS) such as the PODS (Brown et al., 1983). The DMS will support on-line access to selected scatterometer data and will allow the specification of longitude, latitude, and time boundaries of desired data. The requested data will be transmitted to the user either electronically or on magnetic tape. The data available on-line will be as follows:

(1) All wind-field maps

(2) All Level 2.5 data

(3) All Level 2.0 data

(4) A selected 5% of Level 1.5 data for the most recent 12 months

The science investigators and project personnel will determine which regions are included in the 5% of Level 1.5 data that are stored on-line.

In addition to the scatterometer data, the DMS will host *in situ* data for comparison purposes. It may be possible to host certain user data sets that meet format and validation criteria established by the DMS. These *in situ* data will also be available through the on-line selection procedures used for the scatterometer data.

The DMS will have a catalog(s) of available data organized in convenient ways. It will also maintain an on-line bibliography of relevant project and external literature on scatterometry and related subjects.

The DMS will not have the capability for extensive user computing or analysis. The graphics tools available will be mainly for data selection and perusal, not for producing scientific products. Also, there is no plan to use multiple or alternative algorithms in the wind-retrieval processing. Investigators wishing to perform such processing may obtain the Level 1.5 data for their work.

The DMS will archive data (off-line) at several levels. The plan is to archive all of the following:

(1) Data received from the Navy

(2) Level 1.5 data

(3) Level 2.0 data

(4) Level 2.5 data

(5) Wind-field maps

(6) *In situ* data

Since much of the archived data will be stored off-line, an operations staff will be available to extract and distribute selected portions of the archived data in response to users' requests.

D. NSCAT Verification

The wind data from the NSCAT system will be verified in the first year following launch. The goal of the verification will be to quantitatively assess the overall accuracy of the data in terms of location, σ_0, wind speed and direction, and the presence or absence of the rain flag. The sensor (location and σ_0) and geophysical (wind vector and rain flag) verification efforts currently planned for NSCAT are briefly described below. Although the studies described are limited in temporal and geographical extent, similar comparisons are expected to be made between the scatterometer data and the high-quality *in situ* data collected by oceanographic and meteorological field programs such as WOCE and TOGA.

1. Instrument Verification

The σ_0 measurements and location accuracies will be verified using up to three mobile ground monitoring stations, onboard calibration sources, data obtained from σ_0 monitoring cells, isotropic scatterers, and airborne scatterometer measurements. The ground monitoring stations will measure the transmitted power as received on the surface (over land) as the satellite passes overhead. Some additional information on the antenna gain pattern will be obtained from these data. Onboard calibration sources will be used to monitor gain characteristics of the instrument. As shown in Fig. 2, σ_0 cells at an incidence angle of approximately 10° are fairly insensitive to wind speed and direction. Data obtained from cells at this incidence angle will be used to monitor and calibrate σ_0 measurements over the ocean. The backscatter from isotropic scatterers, such as large regions of rain forest, can be used to identify and correct biases in the gain pattern for any individual antenna (Bracalante et al., 1980). Finally, comparisons between measured σ_0 from the NSCAT over the ocean and suitably averaged aircraft underflight measurements of σ_0 will provide direct, if limited, verification of σ_0 accuracy over the ocean under realistic conditions.

A quantitative assessment of σ_0 accuracy will be made within the first six months after launch. However, data for monitoring purposes (ground stations, calibration sources, and isotropic scatterers) will be collected and routinely examined throughout the mission. Level 1.5 data processed in the first six months of the mission will be called "interim" data because the σ_0 validation will not have been completed.

2. Geophysical Verification

To evaluate the accuracy of the geophysical measurements (wind vector and rain flag) the system will be verified by comparing NSCAT winds with winds measured or inferred by conventional, non-NSCAT means. Present plans call for acquiring *in situ* conventional wind data from two experiments conducted at different geographical regions, each lasting approximately two months. The regions will be chosen to encompass a wide range of oceanic and atmospheric conditions. Direct measurements of surface winds will be obtained from buoys (both National Data Buoy Center [NDBC] type moored buoys and drifting buoys), aircraft (such as the National Center for Atmospheric Research [NCAR] Electra or the NOAA P3), and possibly oceanographic ships and instrumented platforms. In addition to direct comparisons between *in situ* and scatterometer winds, plans call for preparing high-quality wind-field maps for the validation regions based on the conventional measurements as well as all other available meteorological information. These maps, which represent an interpolation and smoothing of the wind field, will provide vector wind estimates that can be compared with scatterometer measurements.

Although the direct comparisons discussed above provide an estimate of the intrinsic accuracy of the scatterometer system, many oceanographic and meteorological uses of the data will involve both spatial and temporal averaging of measured winds. As the scatterometer data are irregularly distributed in both space and time, it is not clear how errors in individual measurements will affect averages constructed from many scatterometer measurements. The errors in averaged winds are much smaller than the random errors in the individually measured winds. However, systematic biases, if any, remain in the averaged products. The two-month duration of the system verification experiments, as well as their regional extent (as opposed to isolated point-comparison data sets), will allow estimates of the accuracy of averaged NSCAT data.

The quantitative accuracy of the NSCAT geophysical measurements will be summarized by the end of the first year of the mission. At that time, the NSCAT project, in conjunction with the science investigation team, will determine the necessity for and the nature of any changes to the geophysical model function used to reduce σ_0 measurements to wind vectors. All Level 2.0 and higher level data processed during the first 12 months of the mission will be labeled "interim" data to denote that the geophysical wind products will not have been validated during this period.

Page intentionally left blank

Page intentionally left blank

Section IV
Science Opportunities

A number of oceanographic, meteorological, and scatterometer instrument science studies that could benefit from NSCAT data are identified in this section The specific studies described below are in no way intended to form a complete or comprehensive list. they merely illustrate the range of potential scientific applications of NSCAT data

Although each opportunity is listed under a single heading (oceanographic, meteorological, or scatterometer instrument science), it is clear that many of the studies transcend the boundaries of such an arbitrary classification The ocean responds in many different ways to atmospheric forcing, and the atmosphere in turn responds to changing sea-surface temperature fields. The study of ocean-atmosphere interactions on various scales falls in the provinces of both meteorologists and oceanographers.

Direct measurements of fluxes of momentum (wind stress), heat, and water vapor across the air-sea interface have rarely been made, and no data sets containing *directly* measured fluxes exist for the large space and time scales in which many oceanographers and meteorologists are interested. Instead, fluxes are usually *calculated*, using a parameterization scheme, from bulk measurements of wind velocity and other quantities such as humidity and potential temperature (see, for instance, Large and Pond, 1981) The accuracies of the resulting fluxes depend on both the accuracy of the input data (such as wind velocity) and the validity of the parameterization scheme Details of the formulations of the parameterizations continue to be debated. However, measurements of wind velocity over the oceans have historically been so sparse that calculations of fluxes have been inaccurate principally due to the paucity of bulk wind measurements. Thus, significant scientific progress can be achieved in the study of oceanographic and meteorological problems using flux quantities crudely derived (using parameterization schemes) from the extensive wind *velocity* data to be collected by NSCAT. Many of the scatterometer instrument science studies are aimed at refining the interpretation of scatterometer measurements in light of the important geophysical quantities of interest to oceanographers, meteorologists, and those studying small-scale air-sea interactions.

A. Oceanographic Applications

The ocean is a forced system, and winds are the direct or indirect forcing for many of the most important oceanographic motions. Unfortunately, wind forcing data have never been available in sufficient number or with the accuracy necessary to allow the determination of the detailed dynamic balances governing these motions. Instead, oceanographers have tried to explain observed ocean response in terms of simple hypothetical forcing patterns or have made *ad hoc* adjustments to known forcing data to bring forcing, an ocean model, and ocean data into rough agreement (O'Brien, 1982). Figure 13 illustrates the frequency-wavenumber region of interest to oceanographers and compares the frequency-wavenumber coverage of NSCAT to that of recent studies. Complete and accurate forcing data will make it possible, for the first time, to test the physical ocean models that have been developed. This capability will be greatly enhanced by ocean field programs concurrent with the flight of N-ROSS.

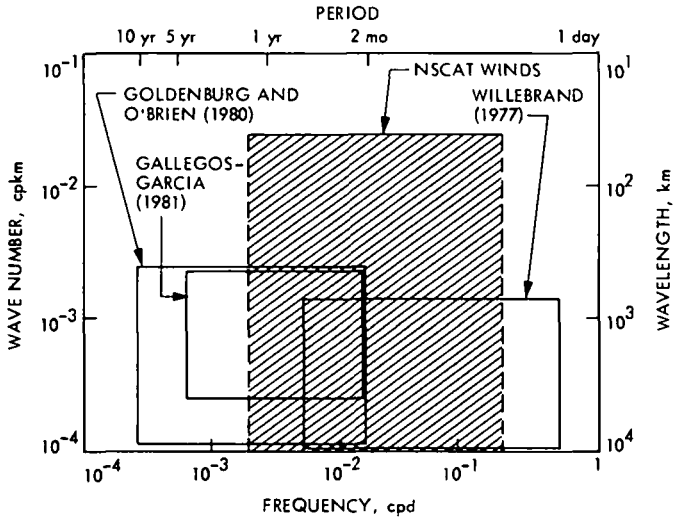

Fig. 13. Frequency-wavenumber region for winds of interest for oceanographic applications, showing coverage of recent studies. Note that the NSCAT data will be useful for characterizing the high-frequency, high-wavenumber portion of the spectrum.

Presented below, in approximate order of ascending temporal and spatial scales, are studies of specific oceanic motions for which NSCAT could provide essential atmospheric forcing data.

1. Mixed Layer Response to Wind Forcing

The surface mixed layer is the link between atmospheric forcing and deeper oceanic motions. In turn, the sea-surface temperature (SST), which is determined by the mixing dynamics of the upper ocean, plays an important role in the exchange of energy between the ocean and the atmosphere. Before the coupled air-sea interaction problem can be tackled, the physics of the ocean mixed layer must be adequately understood and described.

While one-dimensional models (Niiler, 1977) predict that the depth of the mixed layer is governed by wind stirring at the surface and by shearing across the base of the mixed layer

(primarily due to inertial currents), two-dimensional models (deSzoeke, 1980) have shown that Ekman pumping can be as important as turbulent entrainment in determining the mixed layer depth. In addition, wind-driven advection can be important for establishing and intensifying horizontal gradients of SST. It thus appears that three-dimensional models are required to describe the important dynamics governing the mixed layer.

Our ability to construct and test three-dimensional models of the surface mixed layer is severely limited by the lack of adequate wind stress measurements with high spatial resolution. To adequately model the three-dimensional response of the mixed layer beneath a mesoscale atmospheric frontal system, wind observations on a spatial scale of 20 to 50 km are needed. The existence of such data coupled with high-resolution SST and other *in situ* measurements of mixed layer depth and currents should allow critical testing of models and should greatly enhance model development.

Stochastic mixed layer models consider the horizontal variability of SST to be a natural consequence of the stochastic forcing of the ocean by the winds (Frankignoul and Hasselmann, 1977; Frankignoul and Reynolds, 1983). From these models, the spectrum of SST can be predicted from the spectrum of the wind stress. The evaluation of stochastic mixed layer models requires knowledge of the frequency-wavenumber spectrum of wind stress for wavelengths greater than 50 km and for periods greater than about one day. Existing spectral estimates from quasi-geostrophic winds (Willebrand, 1978) and ship winds (Goldenburg and O'Brien, 1980; Gallegos-Garcia et al., 1981) do not have adequate spatial or temporal resolution. Thus, verifying the stochastic models using NSCAT wind data will improve climate modeling of air-sea interactions.

2. Surface Gravity Wave Prediction

Global forecasting of ocean gravity wave directional energy spectra from satellite derived wind fields is a potentially valuable, but little exploited, application of scatterometery. Knowledge of the full two-dimensional ocean wave spectrum is essential in a variety of civil and military applications, such as the prediction of severe, storm-generated waves, the design of offshore structures, the study of beach erosion, and the optimal routing of ships. Although wave-prediction models have evolved considerably since the mid 1950s, none has yet been fully verified with actual field data. The current Northern Hemisphere spectral ocean-wave model in use by the Navy at FNOC does not include swell propagated from the Southern Hemisphere, and indeed, the winds in the Southern Hemisphere are not well enough known to permit either wave forecasts or hindcasts.

The wave field in any ocean region is a function of many variables, the most important of which are as follows:

(1) The recent history of local winds

(2) The winds at earlier times and more distant locations (those that generate swell that may propagate into the region of interest)

(3) Local bathymetry and currents

While the effects of bathymetry and currents appear most important in coastal areas (the Antarctic Circumpolar Current may be an important exception) and are, in any case, reasonably well understood, the largest errors in present global wave-prediction models are attributable to errors in the specification of the wind field, both local and remote (Cane and Cardone, 1981). More accurate predictions of storm location and intensity will lead to more accurate predictions of the wind wave spectrum. The propagation of swell generated by such distant storms can be modeled adequately with present techniques; even more accurate swell predictions could be obtained if the history of winds over the path of the swell were known.

In order to verify wave-prediction models, it is necessary to have both wind-field and wave-field data. NSCAT will allow the necessary wind-field data to be obtained while wave-height data may be obtainable from satellite altimeters such as those on N-ROSS or the Ocean Topography Experiment (TOPEX; a proposed mission dedicated to obtaining altimetric measurements of the ocean surface; the N-ROSS and TOPEX operational lifetimes are planned to overlap significantly). An exciting possibility is the use of data from the European Remote Sensing Satellite ERS-1 (in either the SAR or the wave-spectrometer mode) to estimate two-dimensional wave spectra in the open ocean. Such open ocean wave data would allow wave-prediction models to be evaluated on a global scale as opposed to only in coastal regions or near shipping lanes where adequate conventional wave data are currently available.

3. Dynamics of Midlatitude Current Systems

As reviewed by Fofonoff (1981), our knowledge of the Gulf Stream has been expanded during the last two decades through the development and application of conventional and remote sensing techniques, including instrumented buoys and moorings (Schmitz, 1978) and infrared imaging to map the thermal patterns of the ocean surface from satellites

(Legeckis, 1978). Despite these advances, the dynamic mechanisms by which the Gulf Stream and other major midlatitude current systems form, develop, decay, and finally merge into the large-scale circulation have not been satisfactorily understood. It has not been firmly established whether the path of the Gulf Stream, including its separation from the coast at Cape Hatteras, is controlled by bottom topography (Greenspan, 1963; Pedlosky, 1965; Veronis, 1973), by the distribution of mean wind stress (Strommel, 1948, Munk, 1950, Veronis, 1981), or by mechanisms yet to be determined Leetmaa and Bunker (1978) show that the mean curl of the wind stress reverses sign near Cape Hatteras and is zero over a path that surprisingly resembles the mean path of the Gulf Stream across the western North Atlantic Fofonoff (1981) suggests that the position of the line of zero wind-stress curl may be a consequence, as well as a cause, of the observed Gulf Stream location Harrison (1981) has argued that such a relation between the Gulf Stream and the zero curl may have important consequences for the circulation of the entire subtropical gyre.

Low-frequency variations of the wind-stress curl can force quasi-geostrophic wave motions and variations in the major current systems, such as the Gulf Stream and the Kuroshio. The relationship between the wind-stress curl variations and the oceanic variations has scarcely begun to be examined because only the most rudimentary information about the forcing variations is presently available. Both theoretical and observational (statistical) studies are needed for this entire class of important fluctuations of the ocean circulation. These and other important aspects of large-scale current systems and their relation to the wind can be addressed only when adequate observations of the surface winds over the oceans are available.

4. Midlatitude Midocean Response to Winds

Increased knowledge of wind stress and its curl will improve our understanding of the whole range of oceanic variability in the midlatitudes. Synoptic and mesoscale events in the wind-stress field can force a variety of internal, surface-gravity, and gravity-inertial waves. Lower frequency variations of stress appear to play an important role in the generation of surface fronts.

Inertial-internal and quasi-geostrophic waves may be generated by meso- and synoptic-scale atmospheric systems. Inertial-internal waves generally have periods of slightly less than the local inertial frequency, have horizontal wavelengths of tens to hundreds of kilometers, can have small vertical scales, and may be quite energetic. Because of their large vertical shear, inertial-internal waves very likely contribute to vertical mixing in the ocean (Munk, 1981). Quasi-geostrophic waves have periods ranging from several tens to a few hundred days and wavelengths from a hundred to several thousand kilometers. They have large vertical scales and little vertical shear, but because of their long time scales, quasi-geostrophic waves cause large horizontal particle displacements and contribute substantially to horizontal mixing in the ocean (Rhines, 1977)

Inertial gravity wave generation has been studied for individual forcing events, like the passage of an idealized storm (e.g., Price, 1983), but detailed comparisons of ocean observations with theoretical predictions have never been made, primarily because of uncertainties about the storm-stress field. Calculations of storm surges have rarely been compared in detail to data.

Alternate approaches are stochastic studies, in which a wavenumber-frequency spectrum of stress is used to predict the statistical properties of the current field (e g , Kase and Olbers, 1980). These types of studies have also been limited by a lack of knowledge about the spectrum of stress.

Similarly, both stochastic (Muller and Frankignoul, 1981) and deterministic (Willebrand et al., 1980) models of forced quasi-geostrophic motions have been made Since the curl of the wind stress is the primary forcing for these motions, details of the stress spectrum and forcing pattern can have important effects on the predicted response. The present discrepancies between model results and observations may be due to poor models or inadequate forcing information. Better wind and wind-stress data will help to determine the sources of the discrepancies, which cannot be differentiated at present.

5. Eastern Boundary Current Response to Wind Forcing

Theoretical models of eastern boundary currents all emphasize the importance of wind forcing to the variability of the currents (see Allen, 1980, for a review of wind-driven currents on the shelf). The current variability at any location over the continental shelf is driven not only by local winds but also by winds at locations closer to the equator that force poleward propagating coastal trapped waves. The time scales of wind forcing that are important to currents on the shelf range from the 2- to 10-day time scales that characterize the variability of synoptic scale wind events to the annual scales associated with seasonal variability At sufficiently low frequencies, the current response to fluctuating coastal winds spreads offshore, resulting in a complex system of poleward and equatorward flows. At high frequencies, Rossby wave propagation is no longer possible, and the response to along-shore wind stress

remains trapped at the coast. Although models of eastern boundary current response to winds have advanced considerably in recent years, three-dimensional models capable of examining oceanic response to realistic wind forcing have yet to be developed.

Few quantitative tests of eastern boundary current models have been possible due to a lack of wind data. Clarke (1977) reviews the observational evidence for the existence of wind-generated motions on the continental shelf. While there is some consistency between observations and theory, the model tests are severely limited by the rather poor quality of the observed winds (see also Wang and Mooers, 1977), and it is not at all clear what aspects of the wind field are important to the dynamics. While most three-dimensional models have examined the response to zonally uniform equatorward winds, it is known that a near-shore positive wind-stress curl is associated with these winds. However, neither the length scale nor the temporal variability of this wind-stress curl is known with any reliability, although this near-shore wind-stress curl may be very important to the dynamics of eastern boundary currents beyond the shelf break (Pedlosky, 1974).

What is needed, then, is an accurate characterization of the time and space scales of wind forcing in eastern boundary current regions. To answer all of the scientific questions of interest, measurements of wind stress capable of resolving the energetic 2- to 10-day scales of atmospheric forcing events are required. Although the temporal resolution of the scatterometer measurements is not sufficient for the shorter period synoptic scales, it may be possible to interpolate in time between the scatterometer measurements using high-resolution medium-range forecast models. With wind information available on these time scales, observational studies could be conducted in conjunction with current-meter or sea-level data to quantitatively test models of wind-generated coastal-trapped wave propagation The availability of wind-stress measurements capable of resolving spatial scales on the order of the shelf width (typically 50 km and greater in eastern boundary current regions) would help to guide the development and testing of three-dimensional models of eastern boundary current response to wind forcing

6. Antarctic Circumpolar Current Response to Wind Forcing

The Antarctic Circumpolar Current (ACC) is one of the major current systems in the world oceans In contrast to other major currents, the ACC is unbounded, the water flowing virtually unimpeded (except for the Drake Passage) around the southern ocean between latitudes 45° S and 65° S. In addition, the ACC differs from other major current systems in that the transport of the ACC is highly variable in time, perhaps by as much as 65% of the mean value (Wearn and Baker, 1980).

All analytical and numerical models of the ACC indicate that the flow is primarily forced by winds (e.g., Gill and Bryan, 1971). In contrast to the midocean response to the winds, the zonal wind stress is more important to the dynamics of the ACC than is the wind-stress curl (Munk and Palmen, 1951; Clarke, 1982). A recent model (Clarke, 1982) indicates that for wind forcing with periods less than a few years, the response of the ACC is barotropic. Over these time scales the transport is more strongly correlated with circumpolar-averaged zonal wind stress than with local winds, resulting in fluctuations in the flow that are coherent around Antarctica

There have been few observational studies of the ACC. The mean flow has been mapped from several decades of hydrographic data However, hydrographic data are not adequate to define the seasonal fluctuations of the density field. Current meter measurements at several locations have resolved the temporal variability over time scales up to about a year.

The bottom-pressure measurements of Wearn and Baker (1980) indicate that the flow of the ACC through the Drake Passage may indeed be more coherent with circumpolar-averaged zonal wind stress than local stress, as predicted by the model of Clarke (1982). However, the wind data used by Wearn and Baker are both sparse and of questionable accuracy.

Gaps in our present knowledge of both oceanic and meteorological variability in and above the ACC are enormous We need to learn the dominant time and space scales of the wind forcing in this region and the zonal scales of the current fluctuations. Scatterometer winds will, for the first time, resolve both the temporal and spatial scales of the winds over the ACC. These winds can be used to provide realistic forcing for models. Together with *in situ* measurements from current meters and bottom-pressure gauges, the NSCAT winds will allow detailed statistical studies of the response of the ACC to fluctuations in the wind stress.

A particularly exciting prospect is the possibility of combining NSCAT wind measurements with altimeter measurements of the sea-surface height from an altimeter mission such as TOPEX Since both models and observations suggest that the ACC response to wind forcing is nearly barotropic and of large amplitude, the altimeter could provide reliable measurements of fluctuations in the transport of the ACC

7. Equatorial Ocean Response to Winds and Resulting Climate Fluctuations

The very large changes that occur in the tropical circulations of the ocean and the atmosphere during El Niño-Southern Oscillation (ENSO) events have received much attention in the past decade Observational evidence (Wyrtki, 1975; Barnett, 1977), analytical studies (McCreary, 1976, Moore and Philander, 1977), and numerical simulations (Hurlburt et al., 1976; Kindle, 1979; Busalacchi and O'Brien, 1981) all associate El Niño with low-frequency variations in the wind. In the present models of El Niño, a large amplitude Kelvin wave in the ocean is excited by a relaxation of the zonal component of the surface winds along the equator, and the wave rapidly propagates eastward until its impact with the boundary initiates coastal warming. Since the nature of the response of the equatorial ocean depends critically on the spatial distribution of the surface wind field, it is essential to monitor the detailed structure of the wind field in this region on at least seasonal, annual, and interannual time scales.

In the atmosphere, the Southern Oscillation consists of global-scale fluctuations of atmospheric mass between the Pacific and Indian Oceans. Accompanying these swings of mass are significant changes in the tropical and subtropical wind systems, shifts in atmospheric planetary wave systems, changes in the position of the jet stream, large changes in the rainfall patterns in monsoonal regions and much of the Pacific basin, and remarkable changes in the equatorial current system and the upper ocean heat content of the tropical Pacific. (For a brief review and references, see National Research Council, 1983.)

Evidence suggests that these large-scale oscillations of the atmosphere and the ocean, originating in the tropical regions, are subsequently communicated throughout the global atmosphere, leading to significant interannual climatic fluctuations However, many of the analytical and numerical studies that have been carried out are based on wind fields analyzed from extremely sparse and inadequate data.

The TOGA research program being planned as part of the World Climate Research Program is designed to increase the understanding of events in the oceans and atmosphere that significantly influence the predictability of seasonal to interannual climatic variations over much of the globe. The observational effort is broken down into three components:

(1) Monitoring atmosphere-ocean interactions associated with the ENSO phenomenon over a period of a decade.

(2) Providing a detailed description of a single El Niño episode spanning 15-18 months.

(3) Providing detailed information concerning the processes that control the sea-surface temperature and the fluxes at the atmosphere-ocean interface.

The oceanographic monitoring effort will encompass fluctuations on time scales ranging from weeks to years and will include as one of its objectives a more detailed determination of the climatological mean annual cycle. Major emphasis will be on phenomena with large space scales; therefore, the monitoring network will be sparse but broad enough to cover the entire Pacific basin. The generation (from wind-velocity observations) and analysis of wind-stress fields in the tropical oceans (20° S to 20° N) is an important research activity in conjunction with TOGA. These activities will be centered primarily in the Pacific Ocean, but important activities will be undertaken in the Atlantic and Indian Oceans as well.

Wind measurements from NSCAT could allow the wind-stress field in the entire tropical ocean region to be characterized on spatial and temporal scales far finer than would be possible by conventional means. In addition to defining the major forcing function for equatorial ocean dynamics, these NSCAT measurements would allow examination of some of the detailed mechanisms by which the atmosphere-ocean feedbacks take place in the tropics. It has been suggested that changes in the sea-surface temperature and surface wind convergence are directly linked in some tropical regions. It is, however, extremely difficult to evaluate the surface wind-convergence field from conventional wind data, so the link between the two quantities remains largely speculative. Adequate wind information would permit the study of large-scale air-sea interactions in convergence zones on a variety of spatial and temporal scales. Because the ocean influences the tropical atmosphere largely through the ocean's effect on the location and magnitude of the surface-wind convergence field, understanding better the connections between these two fields is essential to an increased understanding of the coupled ocean-atmosphere problem and to developing an improved predictive capability for ENSO events.

B. Meteorological Applications

Wind measurements are used as both prognostic and diagnostic data in the atmospheric sciences. Although atmospheric observational networks are well established in the Northern Hemisphere over land, little is known about winds in the Southern Hemisphere or over the oceans. The following research topics illustrate some meterological applications of high-resolution measurements of surface winds over the global oceans.

1. Incorporation of Scatterometer Data Into Forecast Models

Experience and analysis have shown that errors in initial conditions can rapidly dominate the solutions and predictions of dynamically based forecasting models. Although the improved accuracy, resolution, and coverage of scatterometers and other remote-sensing instruments *should* improve weather forecasts, Bretherton (1983; private communication) and Baker et al. (1984) conclude that current forecast and general circulation models are not adequate, in resolution and in fundamental surface physics, to dynamically assimilate the vast continuous input of scatterometer wind data. The prospect of operational surface wind data from scatterometers provides significant motivation and opportunity for fundamental model development and optimization. Models must be developed that (1) more realistically account for air-sea interaction and atmospheric boundary-layer processes; (2) assimilate the data in a time-continuous manner; and (3) utilize the unprecedentedly high resolution of scatterometer observations.

On the other hand, mesoscale modeling is highly developed, and some models are already designed to deal with data on the scale of the scatterometer. Some comparative forecast studies with positive results through the use of SASS data have been reported (Guymer, 1983). A detailed case study by Dell'Osso (1983), using the European Center for Medium Range Weather Forecasting fine-mesh model, concludes that high-resolution modeling is capable of improving surface forecasting. (Dell'Osso used high-density Central European surface data for his study and emphasized the general need for high-density data to initialize such models.) NSCAT could provide an extremely large data base with which to develop and test such improved models.

2. Tropical Meteorology

The tropical atmosphere lies primarily over ocean and is poorly represented in the conventional, operational observing system. A number of special international field experiments have been conducted over tropical waters and have contributed to our understanding of many dynamic processes, notably the organization of convection and the relation of smaller to larger scale circulation systems. However, such experiments cannot provide data over large areas or long time periods, and it is clear that routine observations of reasonable resolution are needed to further our understanding.

Scatterometer data may be used to study the dynamics of the planetary boundary layer (PBL) both in extratropical and tropical regions. Information on the vertical structure and momentum transport in the PBL (e.g., Estoque, 1971; Brummer et al., 1974) may be obtained, especially in cloudy tropical regions, by comparing cloud-top movements to surface winds measured by the scatterometer. Two types of approaches compete for modeling the PBL: the so-called modified Ekman theories (e.g., Holton et al., 1971) and the mixed layer theories based on Lilly's (1968) original PBL model. High-quality wind data, to be supplied in part by NSCAT, are needed in order to validate the predictions of these dynamical models.

Though one of the most steady features in the global circulation, the intertropical convergence zone (ITCZ) varies in intensity in space and time, sometimes in a sufficiently regular way so as to show sharp spectral peaks. However, the existing data are not adequate for a complete analysis (Holton et al., 1971), and the wind structure has never been observed over a significant extent of the ITCZ and over an annual cycle or longer.

Another characteristically tropical phenomenon, also on a small scale and too intense for ship observations, is the tropical cyclone. The wind field near the surface surrounding the cyclone is particularly important in that most of the inflow feeding the vertical buildup occurs in the lowest hundred millibars (Shea and Gray, 1973). The great majority of tropical cyclones penetrated by instrumented aircraft have reached relatively northern latitudes. In any event, the lower levels of such storms have never been penetrated by aircraft. Thus, from the point of view of diagnostic studies and modeling, data on the surface wind field for the life of the storm would be of great value.

Finally, there is some indication that the onset of the Indian Monsoon may be correlated with an earlier flow pattern in the Indian Ocean. Some ship reports are usually available, but the data quality and coverage are inadequate. The entire flow pattern around the African continent and the Indian subcontinent requires study and characterization for a succession of monsoon events.

3. Global Circulation and Climatology

Climatology refers in part to statistics calculated in a systematic way and designed to shed light on the dynamics of atmospheric motions. Global statistics are of special interest in leading to conclusions concerning the largest scale general circulation of the atmosphere (Lorenz, 1967). Massive compilations of such statistics are contained in Oort and Rasmussen (1971) for the global atmosphere, and in Newell et al. (1972) for the tropical atmosphere. Large simulation models rely critically on statistical compilations of observations, using them to help define both long-term mean states and the char-

acteristics of shorter term variability (e.g., Manabe et al., 1974). In return, model results are analyzed in order to determine those statistics that play the most crucial role in defining and predicting atmospheric motions. Many compilations of surface-wind or wind-stress statistics (e.g., Han and Lee, 1983) have used decades of data of varying quality in order to obtain the global distribution of mean values. However, large errors are introduced by data errors and data gaps, and few studies have attempted to obtain data for the Southern Hemisphere south of 20° latitude.

The data coverage and quality of NSCAT will begin to permit the study of atmospheric variability on time and space scales hitherto inaccessible by conventional observation systems (although statistically reliable climatologies will require more than the planned three years of data from the N-ROSS mission). These scales of motion will contribute to the statistics and allow quantitative assessments of their importance for the definition and prediction of atmospheric dynamic processes.

4. Case Studies

a. Analysis and prediction of special storms. Already the "Queen Elizabeth II" storm may be the most studied in the history of meteorology, partly owing to the availability of SASS data. The investigation of the development and evolution of unusual storms may provide insights into the principal dynamics for a more general class of atmospheric phenomena.

b. Regional climatology. Circulation patterns that extend to considerable distances offshore vitally affect many areas, notably those dependent on monsoonal rainfall. An accurate climatology is a first step toward understanding the meteorology of the phenomena involved.

c. Southern Hemisphere features. The only meteorological information that we have of vast areas of the Southern Hemisphere is derived from satellite cloud imagery and temperature soundings. Based on SASS data, it appears that there are interesting phenomenological differences between Southern and Northern Hemisphere features. Routine NSCAT observations will provide valuable material for scientific study in this area.

d. Comparisons between NSCAT and cloud-motion winds. Since late 1966, large-scale winds have been inferred by tracking cloud motions based on pictures from geostationary satellites. Although data sets based on these cloud-motion winds thus can potentially span long periods of time and large geographical areas with moderately good spatial resolution, difficulties in determining the cloud height (Whitney, 1983) have led to differences in inferred low-level winds when the same cloud patterns are analyzed by different organizations. Global comparisons between cloud-motion winds and near-surface winds from NSCAT may allow a general quantitative assessment of the accuracy of the historical cloud-motion wind data set. Constructing long time and space series of low-level winds with known accuracy would then be possible for some geographical regions.

e. Atmospheric circulation and the earth's variable rotation. Regarding the earth and the atmosphere together as a system that conserves angular momentum, scientists have accepted that the atmospheric circulation contributes to variations in the earth's rotation (Lambeck, 1980). When upper air networks made possible creditable estimates of total atmospheric momentum, changes in the balance of momentum between the atmosphere and the earth could be calculated and correlated with the appropriate parameters of the earth's rotation. The most elaborate studies to date are those of Hide et al. (1980) and Barnes et al. (1983), in which daily values of the equatorial and axial momentum transfer were compared to changes in the length of day and polar wobble for time spans of up to 16 months. These works concluded that the correspondence is consistent with a causal relationship (see Rosen and Salstein, 1983; Eubanks et al., 1985).

An alternate method of establishing the effects of the atmosphere on the earth's rate of rotation is by directly estimating the torque of the atmosphere on the earth, using surface wind and pressure data. Although momentum transfers have been calculated from surface torque (Newton, 1971a,b), the problems caused by data gaps and the uncertainties of boundary-stress physics have generally been thought to render the budget approach more acceptable. Wahr (1982) suggests calculating torque over oceans, combined with upper wind data over land masses.

The NCSAT data will offer a unique opportunity to determine the stress of the atmosphere on the ocean surface with high precision and fine temporal resolution. By combining NSCAT wind observations over the oceans with observations and calculations from the existing land-based observational network, it may be possible to compare calculations from the two methods, as well as to compare both methods to the rotational parameters, which themselves are now being measured with increased accuracy.

C. Scatterometer Instrument Science Studies

The studies presented in this section are concerned with refining and quantifying the relationship between scatterom-

eter measurements and basic geophysical quantities of interest, such as fluxes of momentum, heat, and water vapor across the air-sea interface. Wind measurements over the ocean have been so sparse that significant scientific progress can be achieved by using flux quantities crudely derived from scatterometer data as an input to oceanographic and meteorological models, as discussed below. Inevitably, however, the models will become more refined, and their sensitivity will make the accuracy of the input an important issue Studies related to the accuracies and interpretations of quantities derived from scatterometer measurements should be pursued prior to and following the N-ROSS mission. Directly comparing satellite-derived quantities and the calculations based on more conventional measurements will help to characterize the relative (as opposed to absolute) accuracies of the calculations and to shed light on the applicability and validity of the physical assumptions used to establish the basic parameterization schemes.

1. Stress Derived from Scatterometer Measurements

Horizontal wind stress is rarely measured directly in an oceanic environment. Instead, the momentum flux from the atmosphere to the ocean is usually calculated from a few bulk measurements of surface wind velocity using a parameterization scheme. The accuracy of the resulting quantities depends both on the accuracy of the input data (the wind observations) and the validity of the parameterization scheme. The values of the drag coefficient(s) and the particular parameterizations have been (and continue to be) generated from temporal averages of wind velocity measured at a point. Since scatterometer winds represent spatial averages (over a footprint) at a given time and since little is known regarding the space-time relationships (if any) governing atmospheric meseoscale motions (c.f. Pierson, 1983a), how to use conventionally generated parameterizations and drag coefficients in conjunction with scatterometer data must be studied in detail (see also Pierson, 1983b)

2. Other Fluxes Using Scatterometer Data

In order to calculate sensible and latent heat fluxes, scatterometer winds must be merged with other satellite data or with synoptic data obtained from ships and buoys. An evaluation of such merging schemes, as well as their accuracies under varying synoptic conditions, will certainly be needed for future oceanographic and meteorological work.

3. Scatterometer-Derived Quantities for Storms

Extratropical and tropical cyclones are regions of high wind speed and are responsible for the events dominating the total momentum transfer from the atmosphere to the upper ocean. In cyclones, the sea state is often not in equilibrium with the wind stress because of changing wind direction and because of the generation of high seas that travel quickly away from the region and become swell.

Several recent studies indicate that drag coefficients based on data obtained in nonstorm conditions are inappropriate for use in storms, but the results are not conclusive (e.g., Byrne, 1982, Geernaert, 1983, K. Davidson, 1983, personal communication). A more comprehensive study is needed.

In high-wind regions, heavy precipitation may interfere with the scatterometer signal. As was described in subsection III.A.6, NSCAT data will be flagged, based on SSM/I-inferred measurements of atmospheric liquid water content, when such atmospheric interference seriously degrades the accuracy of the resulting σ_0 and vector wind measurements. It may be possible for individual investigators to devise corrections for the effects of the liquid water by using simultaneous observations of integrated liquid water derived from brightness temperatures measured by passive microwave sensors. A thorough study of this possibility is in order, since these high-wind regions represent some of the most important situations in which a scatterometer can make significant contributions both operationally and scientifically.

Appendix A

Summary of SASS Results

The Seasat-A Satellite Scatterometer (SASS) was one of five sensors flown aboard the NASA Seasat satellite from 28 June 1978 until the catastrophic failure of the satellite on 10 October 1978. Several review papers have been written addressing aspects of the flight hardware (Grantham et al., 1977, Johnson et al., 1980), data processing (Bracalante et al., 1980; Schroeder et al., 1982, Boggs, 1982), and calibration and geophysical evaluation of the data (Jones et al., 1982; JASIN and GOASEX reports; Brown, 1983). An overall review of SASS can be found in Guymer (1983). In this appendix we concentrate on summarizing the evaluation of SASS accuracy and the scientific use of SASS data. Without a doubt, SASS demonstrated that a satellite-borne, active microwave scatterometer could provide accurate, global, high-resolution measurements of surface winds over the ocean.

A. Evaluation of SASS Accuracy

At the time of its launch, the algorithm used to relate SASS measurements of the normalized radar cross section, σ_0, to wind speed and direction was based on very limited aircraft and satellite (Skylab) data (Moore and Fung, 1979). Two regional field experiments (GOASEX and JASIN), as well as data from operational buoys and weather ships, were used to provide *in situ* measurements of winds for comparison with SASS measurements. Schroeder et al. (1982) describe the evolution and tuning of the geophysical model function resulting in SASS-I, the algorithm used to produce the "official" Geophysical Data Record of SASS winds. As the SASS-I model was tuned to most of the available high-quality *in situ* wind data, little truly independent data exist with which to evaluate the final wind product Nonetheless, comparisons of SASS winds with high-quality JASIN wind measurements and analyzed fields show that SASS winds were accurate to better than ±1.7 m/s and ±17° in direction in the wind speed range 4-16 m/s (Guymer, 1983).

The evaluation studies conducted for SASS graphically illustrated the importance of obtaining high-quality, compatible *in situ* measurements for comparison with satellite wind measurements Most direct *in situ* measurements were temporal averages of point measurements, whereas scatterometer measurements were spatial averages at a single time. As Pierson (1983a) points out, a significant fraction of the rms differences between satellite and *in situ* measurements can be accounted for by the mesoscale variability of the wind field and by the fact that SASS footprints and *in situ* measurements were in general neither colocated nor simultaneous. In Pierson's simplified model, the magnitude of the "mesoscale error" is a function of synoptic scale conditions, the scatterometer footprint size, and the temporal averaging used in the *in situ* measurement

Although SASS data has not (and cannot) add significantly to our knowledge of mesoscale winds with spatial scales smaller than approximately 100 km, the need to calibrate satellite data with *in situ* conventional measurements has focused scientific attention on the importance of mesoscale variability and the proper means of removing its effects from both conventional and satellite data.

B. Utilization of SASS Winds for Numerical Weather Prediction

A number of case studies have been conducted to illustrate the impact of SASS data on Numerical Weather Prediction (NWP) forecasts and analyses (Gyakum, 1980; Cane et al., 1981; Atlas et al., 1982, Baker et al., 1984). It was thought initially that the global, relatively dense coverage of SASS data would provide a much better initial state for NWP models than is available from conventional sources, thus leading to improved forecasting skill. In addition, the ability of SASS data to aid subjective analysis of the model products for short range and regional forecasts (cf. Atlas et al., 1982) was considered to be great.

In fact, the most extensive set of studies of the impact of SASS data on global analysis/forecast models (Baker et al., 1984) showed SASS data had small to negligible positive impact on the accuracy of the forecasts, due mostly to the following:

(1) The difficulty in assigning unique directions to SASS winds (a problem that will be greatly alleviated by the addition of a third antenna on each side for NSCAT).

(2) The inability of current NWP models to fully incorporate surface winds acquired continuously in time, rather than upper-level wind data or surface pressure at fixed synoptic times.

(3) The relative coarseness of the models (4° × 5°) compared with the approximately 0.5° × 0.5° resolution of SASS winds.

All workers have agreed that improved models and data-assimilation techniques, coupled with unambiguous scatterometer vector winds, will lead to more accurate forecasts and analyses.

C. Characterization of Storms and High-Wind Conditions

Hawkins and Black (1983) review SASS measurements of tropical cyclones and storms. Few conventional wind measure-

ments are obtained in gale conditions (wind speeds greater than 17.5 m/s), and there is an almost total lack of data from tropical cyclones. Comparisons between SASS measurements of the extent of gale-force winds and operational advisory predictions revealed several flaws in the forecast advisory values. For example, in 72% of the cases (68) studied, advisories were found to be conservative, that is, the extent of SASS-derived gale-force winds was less than the extent of advisory winds SASS measurements also revealed significant asymmetries in the distribution of gale-force winds about the storm centers, asymmetries which, in general, were not properly accounted for by advisory forecasts. Comparisons between wind measurements from reconnaisance aircraft penetrations of several Atlantic storms indicated that, even in the presence of moderate rain rates, SASS winds had an accuracy of better than ±2 m/s (rms) in gale-force wind conditions. Other studies, notably that by Gyakum (1980) of the "Queen Elizabeth II storm," have demonstrated that SASS winds can be used to accurately place storm centers and determine high wind speeds in otherwise data-poor regions.

D. Oceanographic Applications of SASS Data

The lack of use of SASS data for oceanographic studies deserves specific mention. By far the greatest drawback of the SASS data set is its short duration: most oceanographic phenomena have time scales of weeks to years, and the 100-day duration of Seasat is too short to resolve these phenomena adequately.

In addition, most oceanographic phenomena of interest are sensitive to *vector* winds, not simply wind speed. Although significant progress has been achieved by various groups (most notably that of the group working with Woiceshyn, Wurtele, and Peteherych) in attempting to assign unique wind directions to retrieved winds, a global, 15-day data set (produced by Woiceshyn et al. group) remains the most that has been achieved to this point, although regional sets of unambiguous vector winds exist for isolated passes through the GOASEX and JASIN areas. Examples of temporally averaged vector-wind maps are shown in Figs. 4 and 14.

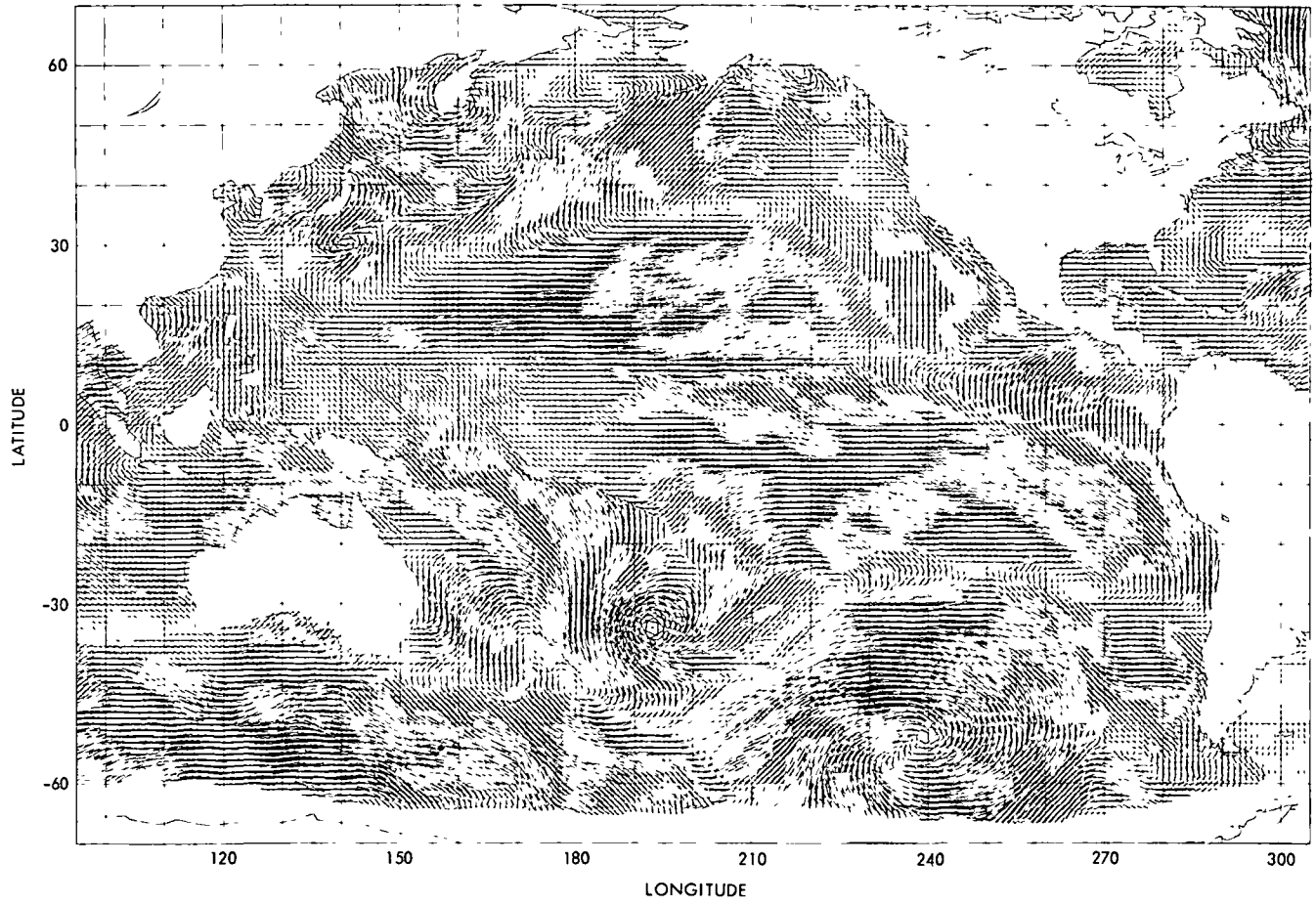

Fig. 14. Vector- and time-averaged wind field from Seasat SASS for the period 6–7 September 1978. Vector wind measurements were interpolated onto a 1° × 1° grid and time averaged (courtesy of P. M. Woiceshyn).

Appendix B

Principles of Scatterometry

A scatterometer is a device that determines the normalized radar cross section (σ_0) of a surface by measuring the backscattered power received when the surface is illuminated by electromagnetic radiation. Microwave scatterometers can be used to measure surface wind speed and direction over the ocean due to an empirically determined correlation between the measured σ_0 of the sea surface and surface winds. This appendix briefly describes the mechanism by which wind speed and direction are determined by scatterometers. More detailed reviews can be found in Moore and Fung (1979), Schroeder et al. (1982), and Pierson (1983b).

A. Radar Scatter at Moderate Incidence Angles

Much theoretical and experimental work since 1950 has established that the dominant source of radar backscatter at moderate incidence angles ($25^\circ \leqslant \theta \leqslant 70^\circ$) is Bragg scatter from small-scale roughness elements on the sea surface (e.g., Wright, 1968, see Fig 15 for a definitional sketch). The wavenumber of the water waves responsible for the Bragg scattering is given by

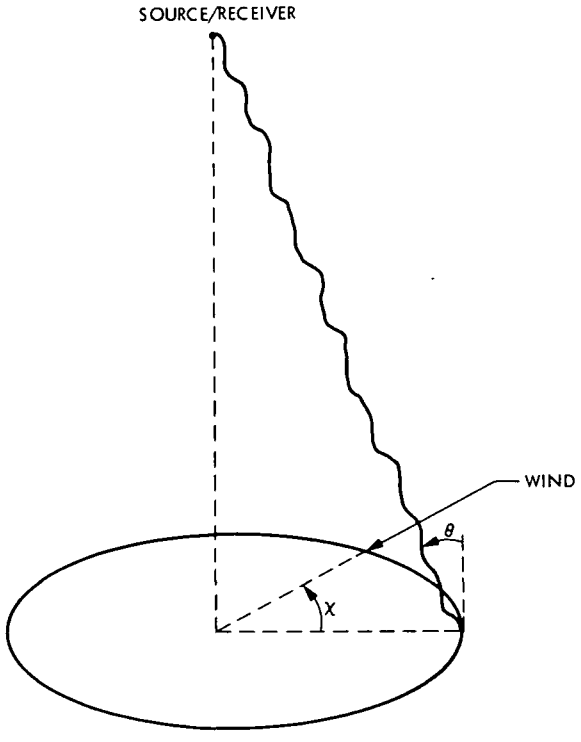

Fig. 15. Definitional sketch of the scattering geometry. Incidence angle θ is measured in the plane normal to the mean ocean surface. Azimuth angle χ is the angle (in the plane of the mean surface) between the wind vector and the projection of the radar illumination vector.

$$k_B = 2k_R \sin(\theta)$$

where $k_B = 2\pi/\lambda_B$; k_R is the wavenumber of the incident radiation, and θ is the incidence angle (vertical angle between the normals to the scattering plane and the illuminating radiation). The amplitude of the backscatter is proportional to the spectral density of the Bragg scatterers (for the NSCAT, Bragg wavelengths range from 2 to 5.5 cm, in the gravity-capillary range), the incidence angle, and the polarization of the incident and scattered radiation. A strong correlation between the spectral density of the short gravity-capillary waves and the local surface winds provides the basis for the interpretation of σ_0 in terms of winds.

Since the ocean surface is composed of waves with many different wavelengths spanning a range from millimeters to hundred of meters, an exact determination of the incidence angle of the illuminating radiation is impossible without knowledge of the detailed shape of the sea surface. However, a two-scale hypothesis (Wright, 1968; Bass et al., 1968), in which locally planar patches ("facets") of Brag roughness elements are tilted relative to the time-averaged mean surface by large-scale waves (with wavelengths much greater than Bragg wavelengths), has been shown to yield accurate predictions of σ_0. When the illuminated area on the sea surface is large compared with even the large-scale waves (as is the case with satellite scatterometers), the average backscatter coefficient at a mean incidence angle (i.e., relative to a flat ocean surface) can be related to the local tilts of the illuminated facets through an average with respect to the slope distribution functions of the large-scale waves (Wright, 1968).

B. Scatterometer Measurement of σ_0

A scatterometer transmits pulses of monochromatic electromagnetic radiation earthward in a fan-like pattern defined by the antennas. Each pulse illuminates an area on the ocean surface and is scattered back to the antennas as described immediately above. Because the scatterometer is mounted on a satellite moving with respect to the ocean surface, the returned signals are shifted in frequency by the two-way doppler effect. Doppler filtering of this backscattered radiation is used to achieve along-beam resolution on the earth's surface, as illustrated in Fig 16 The returned signals are down-converted, amplified, bandpass filtered, and square-law detected. A gated integrator is used to average the output of the square-law detector over a number of returned pulses yielding a measurement $\hat{P}_{s+n}$, where the subscript "$s+n$" refers to the contributions of both the returned signals and the system noise to the measured power. Following this signal-plus-noise measurement, a noise-only measurement, $\hat{P}_n$, is made by integrating the square-law detector output in the absence of radar-return

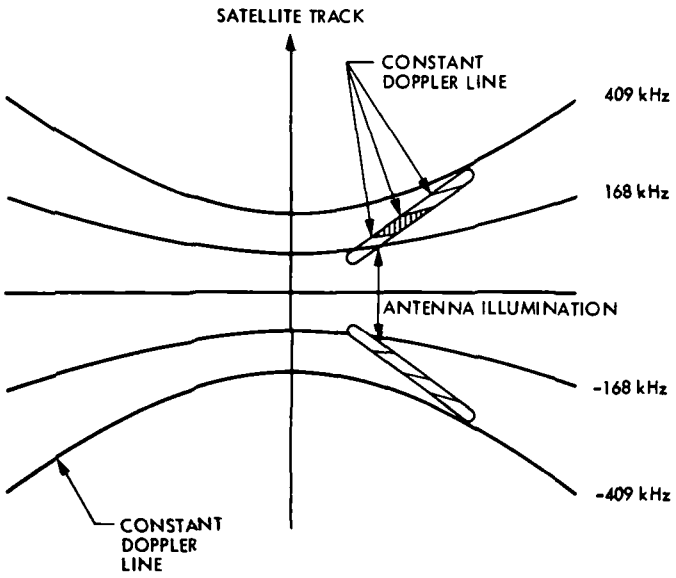

Fig. 16. Geometry of doppler filtering for along-beam resolution. Bandpass filtering selects scattered signals originating between two isodoppler lines on the surface (corresponding to the limiting frequencies of the bandpass filter).

pulses. $\hat{P}_n$ represents an estimate of the average power due to receiver and antenna noise as well as the natural emissivity of the ocean. $\hat{P}_n$ can be subtracted directly from $\hat{P}_{s+n}$ to determine an estimate, $\hat{P}_r$, of the average power in the radar-return pulses; i.e.,

$$\hat{P}_r = \hat{P}_{s+n} - \hat{P}_n$$

Once $\hat{P}_r$ has been determined, σ_0 can be calculated from the radar equation:

$$\sigma_0 = \frac{(4\pi)^3 R^4 L \hat{P}_r}{P_t G^2 \lambda^2 A}$$

where

$\hat{P}_r$ = Power in returned pulse

P_t = Power in transmitted pulse

G = Antenna gain

λ = Wavelength of transmitted signal

A = Effective illuminated area

σ_0 = Scattering coefficient

R = Slant range to illuminated area

L = System losses

The measurement accuracy of σ_0 is affected primarily by communication noise, spacecraft-attitude uncertainty, instrument processing errors (e.g., quantization errors and gain uncertainty), and various bias errors. The bias errors are generally deterministic and are removable, assuming the existence of adequate comparison data. The remaining errors are random in nature and cannot be removed, thus limiting the ultimate measurement accuracy. Of these random errors, those due to instrument processing are relatively minor. Communication noise, a major source of error, is a function of the doppler-filter bandwidth, signal-integration period, and signal-to-noise ratio (SNR). The most significant remaining error source is due to spacecraft-attitude pointing uncertainties. Included are roll, pitch, yaw angle uncertainties due to mechanical and thermal effects, and squint angle (the angle between the electrical and mechanical boresight of the antenna-beam pattern) uncertainty. For high SNR (corresponding to relatively high wind speeds and moderate incidence angles), attitude uncertainties dominate the error. For low SNR (corresponding to low wind speeds and high incidence angles), communication noise dominates. The normalized standard deviation of a σ_0 measurement is the root-sum-square of all random sources of error.

C. Geophysical Model Function

The geophysical model function is an empirical relationship between σ_0 and the wind vector at 19.5 m above the surface in a neutrally stratified atmosphere. The geophysical model function (SASS-I) that resulted from the Seasat mission is specified in the form of a table that gives the two coefficients G and H in the equation

$$\log(\sigma_0) = G(\theta, \chi, \epsilon) + H(\theta, \chi, \epsilon) \log(U)$$

where θ is the radar incidence angle, χ is the horizontal angle between the wind direction and the radar azimuth, ϵ is either h or v (polarization), and U is the neutral stability wind speed at a height of 19.5 m. The quantity σ_0 is a function of the incidence angle, azimuth angle, and polarization; therefore, the G and H coefficients are tabulated separately for v and h polarizations every 2° in incidence angle and 10° in azimuth. These tables thus relate backscatter to wind velocity, given the azimuth and incidence angles. The backscatter varies harmonically with azimuth, with maxima at upwind and downwind and minima at crosswind angles. Figure 3 shows that the functional relationship between σ_0 and azimuth angle χ is nearly $\sigma_0 \approx \cos(2\chi)$. Multiple measurements of σ_0 from approximately the same area on the ocean surface but with different aximuth angles χ can thus be used to determine U and wind direction. The three antennas on each side of NSCAT provide for four different views of the same ocean area, separated by at most a few minutes (depending on incidence angle).

Given the model function, the surface wind speed and direction can be estimated using two or more of the noisy measurements $\hat{\sigma}_0$. Differing algorithms, based on differing assumptions about the statistical properties of $\hat{\sigma}_0$, are currently being investigated. A typical algorithm for estimating wind speed U and wind direction χ (relative to satellite-fixed coordinates) attempts to minimize the residual error between $\hat{\sigma}_0$ and the predicted cross sections for the given U and χ. As a result of the harmonic dependence of σ_0 on χ, the residual error has several local minima. For the case of two noise-free measurements 90° apart, between one and four local minima occur. The set of candidate wind vectors obtained are called "ambiguities." One ambiguity will correspond to the true wind vector, and the others are false solutions. The solutions due to four views from the NSCAT are shown schematically in Fig. 17. In general, the NSCAT configuration allows determination of wind direction with a potential ambiguity of 180°.

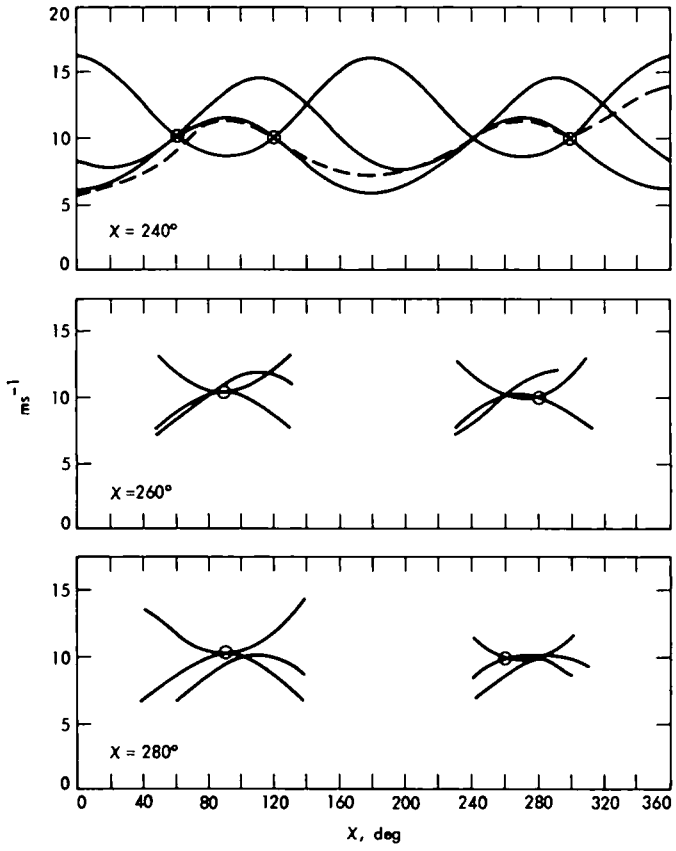

Fig. 17. Simulated speed vs direction solution curves for noise-free data from NSCAT. The SASS-I model function was used in the generation of the curves (after Pierson, 1983b).

Page intentionally left blank

Page intentionally left blank

References

Allen, J.S., 1980: Models of wind-driven currents on the continental shelf, *Annual Reviews of Fluid Mechanics*, 12, 389-433.

Atlas, R , M. Ghil, and M. Halem, 1982: The effect of model resolution and satellite sounding data on GLAS model forecasts, *Mon. Wea. Rev.*, 110, 662-682.

Baker, W.E., R. Atlas, E. Kalnay, M. Halem, P.M. Woiceshyn, S. Peteherych, and D Edelmann, 1984: Large-scale analysis and forecast experiments with wind data from the Seasat-A Scatterometer, *J Geophys. Res* , 89, 4927-4936.

Barnes, R.T.H., R. Hide, A.A. White, and C A. Wilson, 1983. Atmospheric angular momentum fluctuations, length-of-day changes, and polar motion, *Proc R. Soc. Lond* , A 387, 31-73.

Barnett, T.P., 1977: An attempt to verify some theories of El Niño, *J Phys. Oceanogr.*, 7, 633-647.

Bass, F.G., I.M. Fuks, A.I. Kalmykov, I.E. Ostrovsky, and A.D. Rosenberg, 1968: Very high frequency radiowave scattering by a disturbed sea surface, *IEEE Trans. Ant. and Prop.*, AP-16, 560-568.

Boggs, D.H., 1982: *Seasat Scatterometer Geophysical Data Record (GDR) Users' Handbook*, JPL Document 622-232 (internal document), Jet Propulsion Laboratory, Pasadena, CA.

Bracalente, E.M., D.H. Boggs, W.L. Grantham, and J.L. Sweet, 1980: The SASS scattering coefficient (σ^0) algorithm, *IEEE J. Ocean Eng.*, OE-5, 145-153.

Brown, J.W., J.E. Hilland, I.T. Hsu, J.A. Johnson, D.B. Lame, C.L. Miller, and F.J. Salamone, 1983: *Pilot Ocean Data System User Handbook*, JPL Document 715-66 (2 vol.) (internal document), Jet Propulsion Laboratory, Pasadena, CA.

Brown, R.A., 1983: On a satellite scatterometer as an anemometer, *J. Geophys Res.*, 88, 1663-1673.

Brummer, B., E. Angstem, and H. Riehl, 1974: On the low-level wind structure in the Atlantic trades, *Quart. J. Roy. Meteor. Soc.*, 109, 109-121.

Busalacchi, A.J., and J.J. O'Brien, 1981: Interannual variability of the Equatorial Pacific in the 1960s, *J. Geophys. Res.*, 86, 10901-10907.

Byrne, H.M., 1982: *The variation of the drag coefficient in the marine surface layer due to temporal and spatial variations of the surface wind and sea state,* Ph.D. Dissertation, Department of Atmospheric Sciences, University of Washington, Seattle, WA, 119 pp.

Campbell, J.P., 1959: Backscattering characteristics of land and sea at X-band, *1959 Symp. Radar Return, Univ. of New Mexico,* published by Naval Ordnance Test Station, China Lake, CA, as NOTS TP 2338.

Cane, M.A., and V.J Cardone, 1981: The potential impact of scatterometry on oceanography: A wave forecasting case, in *Oceanography from Space*, J.F.R. Gower, Ed., Plenum Press, New York, 587-595.

Cane, M.A., V.J. Cardone, M. Halem, and I. Halberstam, 1981: On the sensitivity of numerical weather prediction to remotely sensed marine surface wind data: A simulation study, *J. Geophys. Res.*, 86, 8093-8106.

Clarke, A.J., 1977: Observational and numerical evidence for wind-forced coastal trapped long waves, *J. Phys Oceanogr.*, 7, 231-247.

Clarke, A.J., 1982: The dynamics of large-scale, wind-driven variations in the Antarctic Circumpolar Current, *J. Phys. Oceanogr.*, 12, 1092-1105.

Dell'Osso, L., 1983 *High resolution experiments with the ECMWF model,* Tech. Report No 37, European Center for Medium Range Weather Forecasting.

de Szoeke, R A., 1980: On the effects of horizontal variability of wind stress on the dynamics of the ocean mixed layer, *J Phys. Oceanogr.*, 10, 1439-1454.

Estoque, M.A., 1971 The planetary boundary layer over Christmas Island, *Month. Wea. Rev* , 99, 193-201.

Eubanks, T.M., J.O Dickey, J.A. Steppe, and P S. Callahan, 1985. A spectral analysis of the earth's angular momentum budget, *J. Geophys Res.*, in press

Fofonoff, N.P., 1981 The Gulf Stream system, in *Evolution of Physical Oceanography*, B.A. Warren and C. Wunsch, Eds., MIT Press, Cambridge, MA, 112-139.

Frankignoul, C., and K. Hasselmann, 1977 Stochastic climate models, Part II: Application to sea surface temperature anomalies and thermocline variability, *Tellus*, 29, 289-305.

Frankignoul, C., and R.W. Reynolds, 1983: Testing a dynamical model for mid-latitude sea surface temperature anomalies, *J. Phys. Oceanogr* , 12, 1131-1145.

Gallegos-Garcia, A., W.J. Emery, R.O. Reid, and L. Magaard, 1981 Frequency-wavenumber spectra of sea surface temperature and wind stress curl in the Eastern North Pacific, *J. Phys. Oceanogr.*, 11, 1059-1077.

Geernaert, G.L., 1983: *Variation of the drag coefficient and its dependence on sea state,* Ph.D Dissertation, Department of Atmospheric Sciences, University of Washington, Seattle, WA. 204 pp.

Gill, A.E., and K. Bryan, 1971: Effects of geometry on the circulation of a three-dimensional Southern Hemisphere ocean model, *Deep-Sea Res.*, 18, 685-721

Goldenburg, S.B., and J.J. O'Brien, 1980. Time and space variability of tropical Pacific wind stress, *Mon Wea. Rev.*, 109, 1190-1207

Grantham, W.L., E.M. Bracalante, N.L. Jones, and J.W. Johnson, 1977: The Seasat-A satellite scatterometer, *IEEE J. Oceanic Eng.*, OE-2, 200-206.

Grant, C.R., and B.S. Yaplee, 1957: Backscattering from water and land at centimeter and millimeter wavelengths, *Proc. IRE*, 45, 976-982.

Greenspan, H.P , 1963: A note concerning topography and inertial currents, *J. Mar. Res* , 21, 147-154.

Guymer, T.H., 1983: A review of Seasat scatterometer data, *Phil. Trans. R. Soc Lond.*, A 309, 399-414

Gyakum, J.R., 1980: On the evolution of the QE II storm, Preprints, *Eighth Weather Forecasting and Analysis Conference,* AMS, Boston, 23-28

Han, Y.-J., and S.-W. Lee, 1983: An analysis of monthly mean wind stress over the global ocean, *Month. Wea. Rev.*, 111, 1554-1566.

Harrison, D.E., 1981: Eddy lateral vorticity transport and the equilibrium of the North Atlantic subtropical gyre, *J Phys. Oceanogr* , 11, 1154-1159

Hawkins, J.D , and P.G. Black, 1983· Seasat scatterometer detection of gale force winds near tropical cyclones, *J. Geophys. Res.*, 88, 1674-1682.

Hide, R., N.T. Birch, L.V. Morrison, D.J. Shea, and A.A. White, 1980: Atmospheric angular momentum fluctuations and changes in length of the day, *Nature*, 286, 114-117.

Holton, J.R., J.M. Wallace, and J.A. Young, 1971: On boundary layer dynamics and the ITCZ, *J. Atmos Sci.*, 28, 275-280.

Hurlburt, H.E., J.C. Kindle, and J.J. O'Brien, 1976: A numerical simulation of the onset of El Niño, *J. Phys. Oceanogr.*, 6, 621-631

Jet Propulsion Laboratory, 1983: NROSS Scatterometer, JPL Proposal, unpublished bound viewgraphs from presentation to NASA on 13 June 1983, available from the NSCAT Project Office, Jet Propulsion Laboratory, Pasadena, CA 91109.

Johnson, J.W., L A. Williams, E.M. Bracalente, F.B. Beck, and W.L. Grantham, 1980· Seasat-A Satellite Scatterometer instrument evaluation, *IEEE J Oceanic Eng.*, OE-5, 138-144.

Jones, W.L., and W.L. Grantham, 1975: Microwave scattering from the ocean surface, *IEEE Trans. Microwave Theory and Tech.*, MTT-23, 1053-1058.

Jones, W.L., and L.C. Schroeder, 1978: Radar backscatter from the ocean: Dependence on surface friction velocity, *Boundary Layer Meteorol.*, 13, 133-149.

Jones, W.L., L.C. Schroeder, and J.L. Mitchell, 1977: Aircraft measurements of the microwave scattering signature of the ocean, *IEEE Trans Antennas Propagat.*, AP-5, 52-61.

Jones, W.L , F.J. Wentz, and L.C. Schroeder, 1978· Algorithm for inferring wind stresses from Seasat-A, *AIAA J Spacecraft and Rockets*, 15, 368-374.

Jones, W.L., L.C. Schroeder, D H. Boggs, E.M. Barcalante, R.A. Brown, G.J. Dome, W.J. Pierson, and F.J. Wentz, 1982: The Seasat-A Satellite Scatterometer: The geophysical evaluation of remotely sensed vectors over the ocean, *J Geophys. Res*, 87, 3297-3317

Kase, R.H , and D.J. Olbers, 1980: Wind-driven inertial waves observed during Phase III of GATE, Suppl I, *Deep-Sea Res.*, 27, 191-216.

Kindle, J.C., 1979: *Equatorial Pacific Ocean variability – Seasonal and El Niño time scales*, Ph D. Dissertation, Florida State University, Tallahassee, FL, 148 pp.

Lambeck, K., 1980 *The Earth's Variable Rotation*, Cambridge Univ. Press, Cambridge, England.

Large, W.G., and S. Pond, 1981. Open ocean flux measurements in moderate to strong winds, *J. Phys Oceanogr* , 11, 324-336.

Leetmaa, A., and A.F. Bunker, 1978· Updated charts of the mean annual wind stress, convergences in the Ekman layers and Sverdrup transports in the North Atlantic, *J Mar. Res* , 36, 311-322.

Legeckis, R., 1978. A survey of worldwide sea surface temperature fronts detected by environmental satellites, *J. Geophys. Res.*, 83, 4501-4522.

Lilly, D.K., 1968: Models of cloud-topped mixed layers under a strong inversion, *Quart. J. Roy. Meteor. Soc* , 94, 292-309.

Lorenz, E.N., 1967 *The nature and theory of the general circulation of the atmosphere*, W.M.O., TP 115, Geneva, Switzerland

Manabe, S., D.G. Hahn, and J.L Holloway, 1974 The seasonal variation of the tropical circulation as simulated by a global model of the atmosphere, *J. Atmos. Sci*, 31, 43-83.

McCreary, J.P., 1976· Eastern tropical ocean response to changing wind systems: With application to El Niño, *J Phys. Oceanogr.*, 6, 632-645.

Moore, D.W., and S.G.H. Philander, 1977 Modeling of the tropical oceanic circulation, in *The Sea*, VI, E.D. Goldberg, Ed., Wiley Interscience, New York, 319-361.

Moore, R.K., and W.J. Pierson, 1966 Measuring sea state and estimating surface winds from a polar orbiting satellite, *Proc International Symp. on Electromagnetic Sensing of the Earth from Satellites*, Miami Beach, Florida, R1-R28.

Moore, R.K., and A.D. Fung, 1979: Radar determination of winds at sea, *Proc. IEEE*, 67, 1504-1521.

Muller, P., and C. Frankignoul, 1981: Direct atmospheric forcing of geostrophic eddies, *J. Phys. Oceanogr.*, 11, 287-308.

Munk, W.H., 1950 On the wind-driven ocean circulation, *J. Meteor*, 7, 79-93.

Munk, W.H., 1981: Internal waves and small-scale processes, in *Evolution of Physical Oceanography*, B.A. Warren and C. Wunsch, Eds., MIT Press, Cambridge, MA, 264-291.

Munk, W.H., and E. Palmen, 1951: Note on the dynamics of the Antarctic Circumpolar Current, *Tellus*, 3, 53-56.

National Research Council, 1983: *El Niño and the Southern Oscillation. A Scientific Plan*, National Academy Press, Washington, D.C., 72 pp.

Newell, R.E., J.W. Kidson, D.G. Vincent, and G.J. Boer, 1972: *The General Circulation of the Tropical Atmosphere* (2 vol.), MIT Press, Cambridge, MA.

Newton, C.W., 1971a: Mountain torques in the global angular momentum balance, *J. Atmos. Sci.*, 28, 623-628.

Newton, C.W., 1971b· Global angular momentum balance: Earth torques and atmosphere fluxes, *J. Atmos. Sci.*, 28, 1329-1340

Newton, R.W., and J.W. Rouse, Jr., 1972: Experimental measurements of 2.25-cm back-scatter from sea surfaces, *IEEE Trans. Geosci. Electron.*, GE-10, 2-7.

Niiler, P.P., 1977. One dimensional models of the seasonal thermocline, in *The Sea*, VI, E.D. Goldberg, Ed., Wiley Interscience, New York, 97-115

O'Brien, J.J., Ed., 1982: *Scientific Opportunities Using Satellite Wind Stress Measurements over the Ocean*, NOVA University/N.Y.I.T. Press, Fort Lauderdale, 153 pp.

Oort, A.H, and E.M. Rasmusson, 1971: *Atmospheric circulation statistics,* NOAA Professional Paper 5, Washington, D.C.

Pedlosky, J. 1965: A necessary condition for the existence of an inertial boundary layer in a baroclinic ocean, *J Mar. Res.*, 23, 69-72.

Pedlosky, J., 1974. Longshore currents, upwelling and bottom topography, *J. Phys Oceanogr*, 4, 214-226.

Peteherych, S., M.G. Wurtele, P.M. Woiceshyn, D.H. Boggs, and R.R. Atlas, 1984: First global analysis of Seasat scatterometer winds and potential for meteorological research, Paper presented at the URSI Commission F Symposium and Workshop, Shoresh, Israel.

Pierson, W.J., 1983a: The measurement of the synoptic scale wind over the ocean, *J. Geophys. Res.*, 88, 1683-1708.

Pierson, W.J., 1983b: Highlights of the Seasat-SASS program: A review, in *Satellite Microwave Remote Sensing*, T.D. Allan, Ed., Halstead Press, New York, 69-86.

Price, J.F., 1983: Internal wave wake of a moving storm. Part 1: Scales, energy budget and observations, *J. Phys. Oceanogr.*, 13, 949-965.

Rhines, P.B., 1977: The dynamics of unsteady currents, in *The Sea*, VI, E.D. Goldberg, Ed., Wiley Interscience, New York, 189-318.

Rosen, R.D., and D.A. Salstein, 1983: Variations in atmospheric angular momentum on global and regional scaless and the length of day, *J. Geophys. Res.*, 88, 5451-5470.

Ross, D., and W.L. Jones, 1978: On the relationship of radar backscatter to wind speed and fetch, *Bound. Layer Meteorol.*, 13, 133-149.

Schmitz, W.J., Jr., 1978: Observations of the vertical distribution of low frequency kinetic energy in the Western North Atlantic, *J. Mar. Res.*, 36, 295-310.

Schroeder, L.C., D.H. Boggs, G. Dome, I.M. Halberstam, W.L. Jones, W.J. Pierson, and F.J. Wentz, 1982: The relationship between wind vector and normalized radar cross section used to derive Seasat-A Satellite Scatterometer winds, *J. Geophys. Res.*, 87, 3318-3336.

Shea, J., and W.M. Gray, 1973: The hurricane's inner core region, *J. Atmos Sci.*, 30, 1544-1564.

Stommel, H., 1948: The westward intensification of wind-driven ocean currents, *Trans Amer. Geophys. Union*, 29, 202-206.

Valenzuela, G.R., M.B. Laing, and J.C. Daley, 1971: Ocean spectra for the high frequency waves as determined from airborne radar measurements, *J. Mar. Res.*, 29, 68-84.

Veronis, G., 1973: Model of world ocean circulation. Part I: Wind driven, two layer, *J. Mar. Res.*, 31, 228-288.

Veronis, G., 1981: Dynamics of large-scale ocean circulation, in *Evolution of Physical Oceanography*, B.A. Warren and C. Wunsch, Eds., MIT Press, Cambridge, MA, 140-183.

Wahr, J.M., 1982: The effects of the atmosphere and oceans on the earth's wobble, Part I: Theory, *Geophys. J. R. Astr. Soc.*, 70, 349-372.

Wang, D.P., and C.N.K. Mooers, 1977: Long coastal-trapped waves off the west coast of the United States, summer 1973, *J. Phys. Oceanogr.*, 7, 856-864.

Wearn, R.B., and D.J. Baker, 1980: Bottom pressure measurements across the Antarctic Circumpolar Current and their relation to the wind, *Deep-Sea Res.*, 27A, 875-888.

Whitney, L.F., 1983: International comparison of satellite winds – An update, *Adv. Space Res.*, 2, 73-77.

Willebrand, J., 1978· Temporal and spatial scales of the wind field over the North Pacific and North Atlantic, *J Phys Oceanogr* , 8, 1080-1094

Willebrand, J , S.G H. Philander, and R.C. Pacanowski, 1980. The oceanic response to large-scale atmospheric disturbances, *J Phys. Oceanogr.*, 10, 411-429.

Wiltse, C J , S.P. Schlesinger, and C.M. Johnson, 1957. Backscattering characteristics of the sea in the region from 10 to 50 kMc, *Proc IRE*, 45, 220-227.

Wright, J W., 1968. A new model for sea clutter, *IEEE Trans. Ant and Prop* , AP-16, 217-223.

Wyrtki, K., 1975 El Niño – The dynamic response of the equatorial Pacific Ocean to atmospheric forcing, *J Phys Oceanogr.*, 5, 572-584.

Young, J.D., and R.K. Moore, 1977. Active microwave measurement from space of sea-surface winds, *EEE J. Ocean Eng* , OE-2, 309-317.

NASA—JPL—Coml L A . Calif